Design of Shape-Transforming Canopies for Parachutes

A Major Qualifying Project report
submitted to the Faculty of

WORCESTER POLYTECHNIC INSTITUTE

in partial fulfillment of the
requirements for the degree of

Bachelor of Science in Aerospace Engineering

by

Amanda L. Pollack '09

Kyle H. Miller '09

Casey M. Rogan '09

Jeffrey S. Moffett '09

April 30, 2009

Date

Prof. David J. Olinger, advisor

Project number ME-DJO-0309

ABSTRACT

Design of a single-parachute cargo delivery system that can significantly alter its glide slope and descent characteristics via mid-flight shape transformation can reduce costs and simplify cargo drops. Current systems use multiple canopies to deliver cargo to a predetermined drop zone. From twelve design concepts invented by this team, two were chosen for development based on given constraints, and were tested through computer simulation and real-world experiments. Developing two parallel transformation concepts has permitted the comparison of key performance parameters. In addition to the canopies, a servo-based remote-controlled command system was designed and manufactured to initiate the transformation. Drop tests from a Black Hawk helicopter at 300 feet AGL showed that, with further study and research, a single-parachute cargo delivery system could be a viable alternative to the systems currently in use.

ACKNOWLEDGEMENTS

The U.S. Army Soldier Systems Center in Natick, Massachusetts has provided literature, materials, and funding for this project. Numerous other projects involving parachutes have also been completed at Worcester Polytechnic Institute in conjunction with the Center in previous years. Our project is a continuation of past work, integrating lessons learned into our design, and we acknowledge the work done by previous project groups.

We would also like to thank Professor David Olinger, Justin Riley, Jim Sadeck and the U.S. Army Soldier Center for their thorough guidance and generous contribution of resources throughout this project.

TABLE OF CONTENTS

TABLE OF FIGURES

NOMENCLATURE

α	angle of attack
AGL	above ground level
AR	aspect ratio
b	span of parafoil
C_D	coefficient of drag
C_L	coefficient of lift
C_r	resultant force coefficient
CAD	computer-aided design
d	parachute canopy diameter
D	drag force
g	gravitational acceleration
GPS	global positioning system
k	air resistance constant ($k = \frac{1}{2}\rho S_o C_D$)
L/D	lift-to-drag, glide ratio
m	total mass of the system
μ	kinematic viscosity of air
ODE	ordinary differential equation
Re	Reynolds number
ρ	density of air
S_o	total fabric surface area
S_p	area of side panel in parafoil
S_w	area of upper surface of parafoil
t	time
V	descent velocity
V_t	trajectory velocity
W	total weight of the system
w	width of parafoil

I. INTRODUCTION

THIS PROJECT HAS ENDEAVORED to design a viable parachute cargo delivery system with the ability to significantly alter its glide slope and descent characteristics using a mid-air canopy transformation. Systems currently in use typically employ two separate parachute canopies, the first being a high lift-to-drag ratio (L/D) parafoil that enables the cargo system to steer itself to a predetermined drop zone using GPS. High L/D also translates to a shallow glide slope, permitting cargo to be deployed many miles from a chosen target, with the deployment aircraft ideally out of range of enemy weapons. After the parafoil approaches its target, a second parachute, usually a round canopy with a low L/D, is deployed while the first deflates. This canopy allows the cargo to descend gently to the ground and limits damage from dragging at impact.

Our goal has been to devise a single parachute canopy that could replace and thereby reduce the cost of these current systems. After inventing and reviewing twelve unique concepts for how such a transformation could be undertaken, we selected the two most promising design concepts and sized them to the payload design constraint we had been issued, a maximum cargo weight of five pounds. A five-pound sensor payload would be useful in military surveillance and reconnaissance applications, especially in tracking enemy vehicular movements. Developing two transformation concepts in parallel has permitted the comparison of canopy flight and performance characteristics, to aid in the ultimate selection of the best design.

In addition to our own innovations to permit transformation, canopy design and sizing were based on a literature review of earlier work on parachute design. Two working parachute canopies have been constructed from porous and non-porous rip-stop nylon parachute fabric. Both completed canopies have undergone testing in their gliding and vertical descent modes, using high windows in WPI campus buildings as a launch point; in an open wind tunnel made from an adapted industrial fan; and in a final drop test from a UH-60 Black Hawk helicopter. Closed wind tunnel testing has also been conducted with a

force balance to experimentally determine the drag coefficients of certain prototype canopy designs.

A servo-based remote-controlled transformation system was also designed and constructed, enabling both canopies to transform on command during testing. The system can reliably effect a major canopy transformation with only a small action at the location of the suspended payload, and thus offers significant advantages in its simplicity and repeatability of operation.

The U.S. Army Soldier Systems Center, in Natick, Massachusetts provided literature, materials, and funding for this project. A generous offer by the Center also made possible our final drop test from a U.S. Army helicopter.

Project definition

"An airdrop of military personnel and equipment is the final phase of transport to a theater of operation. Personnel and equipment must land uninjured, undamaged, and ready for action or use."[2] The U.S. military has developed multiple systems to achieve this end. For mid-sized cargo loads of about 10,000 pounds, the U.S. Army currently uses a system called SCREAMER, which is depicted in Fig. 1.

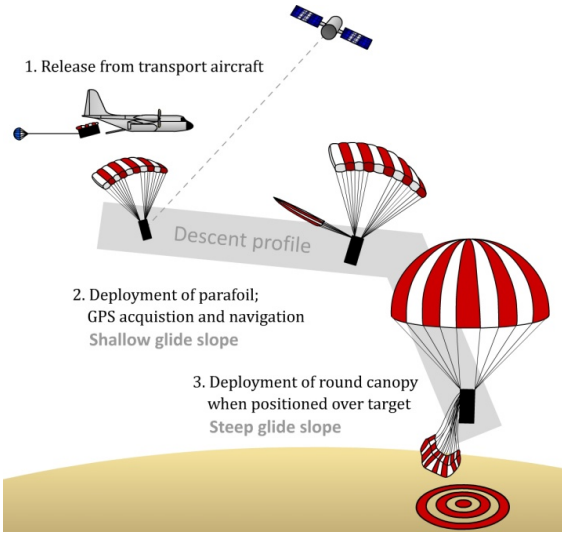

Figure 1: A schematic of the SCREAMER system currently employed by the U.S. Army (adapted from Ref. 1)

This system employs a two-parachute design. The first of the two parachutes used is a parafoil, which has a higher, wing-like lift-to-drag ratio (L/D) to better enable the cargo system to steer itself, using GPS, to a predetermined drop zone. High L/D also translates to a shallow glide slope, permitting cargo to be dropped many miles from the target, often out of range of enemy weapons. After the cargo is near the desired location, a second parachute is

deployed while the first deflates. The second parachute is a round canopy with a lower L/D, which allows the system to descend more vertically while minimizing drift from its desired position over the target. This multi-parachute system, while effective, is complicated and expensive.

Our goal has been to devise a single parachute canopy and mechanism that could replace the current SCREAMER system. To accomplish this, a system that transforms the *shape* of the parachute canopy was desired. This open-ended design problem has allowed us to innovate and produce a single-parachute system that, should the U.S. Army choose to develop it more fully, could be less expensive and easier to field-rig than the SCREAMER system, and even more readily scalable to multiple weight categories.

Project objectives

The overall objective of this project has been to design and construct at least one working parachute canopy that can transition mid-flight from a high-L/D gliding canopy to a low-L/D canopy for steep but gentle descent, in order to effectively deliver a five-pound payload to a theoretical target. The constraint of five pounds was not arbitrarily chosen, but was instead chosen by our sponsor as a rough specification for a payload of logistical value to the U.S. Army.

Such a payload could include a GPS parachute navigation system, actuators to steer the canopy and trigger the transformation, a set of accelerometers to monitor the system's surroundings after landing, and a communication unit for relaying status and observations to headquarters. The thinking behind such a "smart rock" payload, especially one camouflaged to blend in with the terrain, is that it would be able to detect and communicate the presence of enemy vehicles cheaply and effectively, especially if deployed in large numbers over a wide area.

To achieve our objective, we identified several project goals, discussed in more detail on the following page.

Goal 1: Conduct a literature review

To learn about the challenges involved in parachute design, we researched a variety of current systems, concentrating on the descent performance of round and gliding parachutes, wind tunnel testing, and a general history of the parachute.

Goal 2: Design and construct several models for testing purposes

We brainstormed twelve designs for our model. After preliminary analysis and a practicality assessment of each design in light of our cargo requirements, we narrowed our focus to two designs to permit comparative testing and analysis throughout the design process.

Goal 3: Conduct tests and analyze results

We have tested our models in wind tunnels and with drop tests to select and quantify the properties of the final design. The data collected from testing has been analyzed with respect to vital parachute performance parameters, e.g., descent velocity, glide slope, and L/D.

II. BACKGROUND

Hoping to garner some insight into the peculiarities of parachute design, we briefly studied the storied history of the parachute. More practical information was obtained, however, from a review of current parachute-based cargo delivery systems.

History

The history of the modern parachute is surprisingly short. However, the concept of using air resistance to retard one's fall has a much longer history. Compared to other conceptually difficult forms of flight like the airplane, parachutes operate on the intuitive principle of wind-resistance, and in a manner accessible to any civilization that used textiles (e.g., those who could sail). As a result, they were relatively common in the more technologically advanced civilizations of China and Siam in the late Middle Ages.[2]

"Tragedy has been a constant companion of the parachute."[3] From its earliest documented use, faulty parachutes, whether improperly sized, poorly constructed, or designed according to some fundamentally incorrect interpretation of the laws of Nature, have been quick to cause injury and death to those foolish enough to use them without adequate testing. In just one example, more than 800 years ago in Constantinople, Byzantine emperor Comnenus was visited by a Turkish sultan who proposed to demonstrate a parachute by jumping from a tower. His device failed to work, causing him to break "every bone in his body."[3]

If every jump had been fatal, development of the parachute would have eventually ceased altogether. There were some successes, then, many arising from the scientific advances of the Renaissance. Leonardo da Vinci is known for his parachute design of 1485 (*Codex Atlanticus*), and others developed similar designs in this time period.[3] In 1595, Faust Vrančić, a Hungarian scientist living in Italy, tested a design by jumping from a church bell-tower in Venice. His concept is illustrated as *HOMO VOLANS* , the "flying man", in his book of inventions, *Machinae Novae*. He went on to live another 22 years, so one can assume his invention worked reasonably well.[3]

A Siamese entertainer used parachutes in the 17th century to earn the favor of his king, who made him a "great Lord."[3] The 18th century saw increasing popularity of the parachute in entertainment. In 1783, Louis-Sébastien Lenormand, a French scientist and the inventor of the word *parachute*, jumped from the tower of Montpellier Observatory with a 14-foot-wide cone-shaped parachute.[3] His attempt, witnessed by a crowd of onlookers, provided inspiration to future innovators in France.

Continuing in Lenormand's footsteps, Frenchman Jean-Pierre Blanchard used parachutes in 1794 in a variety of experiments, testing his designs by dropping animals from different heights.[3] André-Jacques Garnerin, perhaps inspired by Blanchard and Lenormand, jumped from a hydrogen-filled balloon with a parachute. As went one contemporary account:

> When he reached a height of 3,000 feet he cut the cords which held the parachute to the balloon…The latter exploded and the parachute began to descend with such rapidity that a cry of horror escaped from the spectators and several ladies fainted.[3]

Garnerin survived, however, his parachute performing its duty admirably. Others in his era had varying degrees of success. In 1793, a French general named Bournonville was sent to prison in the Czech Republic, where he attempted to escape from his cell by jumping out of the window with an umbrella. His impromptu parachute broke his 40-foot fall, allowing him to survive with only a broken leg. However, he was promptly carried back into the prison and given more time in jail for his attempted escape.[3]

In April of 1790, an English "man of science" named Murray parachuted from the bell-tower of Chichester Cathedral, was overturned by a wayward gust of wind, and "fell to the ground with great force, blood gushing from his ears, nose and mouth, very plentifully, and was unconscious for hours."[3]

The modern parachute, at last beginning to serve its present-day purpose rather than that of pure entertainment, saw a landmark flight in 1802, when Pole Jordaki Kuparento jumped from his "fire balloon," which had incidentally gone up in flames, and landed safely on the ground.[3] This was the first time the parachute had saved a life.

More than one hundred years later, in 1910, Captain Albert Berry jumped from an airplane, arguably the first time a parachute had been used from an aircraft traveling at any appreciable velocity.[3] The practical use for this invention was beginning to be seen, and with the advent of the First World War four years later, its value in combat was soon to be tested.

The Germans were the first to begin using parachutes in the final year of WWI. Some Allied pilots "regarded [parachutes] with contempt, as if carrying a parachute were an admission of weakness." As one put it, "a pilot's job is to stick to his aeroplane."[3] Others would have used parachutes if provided, but often conflicting priorities meant that pilots were rarely equipped with them. One R.A.F. pilot, Second Lieutenant Leslie Pargeter, said of the R.A.F.'s R.E.8 biplanes: "In these planes, fire was our third passenger. If we'd caught fire and had parachutes, we'd have used them. But of course, we never had them."[3]

Parachutes were also becoming popular in the United States during this period. Inspired by a parachute maker's demonstration, Charles Lindbergh became an early adopter of the device, at first using it in his barnstorming demonstrations. The parachute later saved Lindbergh's life, however, and he "became the first man known to have his life saved twice by a parachute, which earned him special status in an unofficial fraternity created by the Irvin Parachute Company called the Caterpillar Club."[4]

World War II witnessed the adoption of the parachute by both the Axis and the Allies "in practically every theatre of war."[3] Its extensive use allowed designers to identify previously unknown properties of the parachute. They discovered that if a parachute was deployed at too high a speed, it would "squid" and fail to open. They also observed the effects of canopy fabric porosity; too low a porosity would cause oscillation of the parachute during descent. New materials were researched and developed, silk being harder to obtain during the material shortages of wartime. Some alternatives included nylon, rayon and even parachute cloth woven from paper thread.[3]

During the six years of WWII, the parachute went from being able to deliver a mere 150 pounds of supplies in 1939 to jeeps and heavy artillery suspended from multiple canopies on D-Day.[3] Parachutes were used to drop sea-mines and landmines that would explode after a silent drop to earth, to recover practice rockets, and to slow the fall of

reconnaissance flares. One of the more innovative naval uses was the "parachute-and-cable rocket," which launched a metal cable, anchored to a ship's deck, into the path of an enemy aircraft, where it was hoped that the wire, suspended by parachute, would tear off an attacker's wing.[3]

In the half-century or so since WWII, parachutes have returned to their longtime original purpose, entertainment. Sport parachutes made from rip-stop nylon are used by sport parachuting amateurs and veterans alike. New designs emerged in the 1960s, with inventors adapting the principles of the aircraft wing to create parafoils and other shapes that could fly at great forward speeds with gliding performance approaching that of some airplanes. Parachutes are now used in diverse circumstances: smoke jumping, delivering survival equipment to stranded hikers, decelerating aircraft and ground vehicles, and recovering missiles and rockets.[2] They can be deployed at speeds in excess of Mach 4, in the upper reaches of the atmosphere, and supporting payloads of 185,000 pounds.[2]

Modern systems

The U.S. military has developed a wide variety of parachute systems for use in air drop resupply. For example, the Precision and Extended Glide Airdrop System ("PEGASYS") is a system consisting of a canopy, airborne guidance unit, and pallet platform. It is currently in use in combination with the Precision Airdrop System ("PADS") to form the Joint Precision Airdrop System ("JPADS"). PADS is an onboard computer system designed to estimate the release point for high altitude cargo drops.

JPADS combines the best of both of these systems into an improved air-drop delivery system, and is jointly owned by the Army and the Air Force. It can adjust in real

Figure 2: The PEGASYS system[5], JPADS system[6], and Sherpa system[7], respectively.

Figure 3: The LVAD System[9] and a CDS bundle[10] being loaded onto an aircraft.

time to changing conditions and targets, making it a valuable tool for quick resupply when properly matched to the delivery aircraft's range and speed. JPADS gives more release flexibility to the pilot and reduces load dispersion on the ground to a radius of approximately 100 meters. The system serves four main objectives: it increases ground accuracy, permits standoff delivery, increases delivery aircraft survivability, and provides better information back to the controller. JPADS is designed to only handle loads between 10,000 and 42,000 pounds, but systems to handle smaller loads between 2,200 and 10,000 pounds are currently in development. [8]

"Sherpa" is a temporary system currently in use while JPADS is more fully developed. Sherpa consists of a 900-square-foot ram-air canopy, parachute control system, GPS unit, and mission planner. The system can handle up to 1,200 pounds of cargo, and can be dropped as high as 25,000 feet and as far away from the target as nine miles (also known as "standoff delivery"). The mission planner is programmed ahead of time with the drop zone location, the aircraft's altitude and speed, cargo weight, and wind speeds at various altitudes. It then calculates a flight plan and the exact point in the sky that the system must be dropped. If desired, obstacles to be avoided can also be programmed into the flight planner. With Sherpa, the pilot does not need to make visual contact with the drop zone, and cargo can be dropped in almost any weather or time of day. Sherpa is nearly

autonomous, and when used properly can land itself within 200 meters of the intended drop zone.[11]

Other systems in use are the Low Velocity Air Drop ("LVAD"), the Container Delivery System ("CDS"), and in the past, the Low Altitude Parachute Extraction System ("LAPES"). LVAD is a system used to drop cargo from 500 feet or more above the ground. It is designed to handle payloads from 2,200 pounds to 60,000 pounds, and lands cargo at a velocity less than 28.5 feet per second. This system consists of an extraction parachute and a recovery parachute. LVAD helps to increase accuracy of aerial delivery systems, reduces load dispersion, and increases aircraft and equipment survivability by placing the aircraft below high-risk zones for anti-aircraft weapons.

CDS is a cargo support system designed to be used in conjunction with another system like LVAD. It uses gravity to extract payloads, and consists of a platform and cargo restraints. The size of the platform depends on the size of the air carrier's cargo hold. It can handle anywhere from 500 pounds to 2,200 pounds, and is the system most commonly in use today.

Used heavily in Vietnam, LAPES can deliver cargo up to 38,000 pounds. Designed to be extracted from an aircraft flying only five to ten feet off the ground, LAPES uses a 15-foot drogue chute to pull pallets out of an airplane's rear cargo door. Upon impact, the pallet is slowed to a stop by friction with the ground. Due to the dangers associated with this extreme closeness to the ground and evolving war tactics, this system is no longer in widespread use in the military.[11]

Figure 4: The LAPES System[12]

Model scaling

After some consideration, and especially in light of the reasoning behind our sponsor's payload specification, we made the decision to not attempt to scale down a large parachute, but instead simply design a small parachute from scratch. Rather than confront the potentially difficult and nonlinear problems of canopy size and payload weight scaling, we have chosen to treat our sponsor's five pound payload specification as an absolute design goal, rather than interpreting it as "a 5,000-lb vehicle *scaled to* 5 lb."

On the other hand, we believe that scaling *up* our system for larger payloads, should it someday be desirable, is best left to parachute experts. As will be seen later, our transformation methods work well for small payloads but will likely require a redesign for heavier cargo deliveries.

III. METHODOLOGY

Our design process was iterative. From the invention of possible transformation methods, to experimentation with various rigging schemes, to the design of our servo control mechanism, virtually every stage in our project involved some aspect of trial, error and adjustment. The following sections discuss the process of inventing, sizing, constructing and testing our two final parachute canopies.

Design constraints

A number of constraints affected our design process. As previously stated, our maximum payload weight limit was set at five pounds by our sponsor. Additionally, as per U.S. Army specifications, our cargo could have a maximum vertical impact velocity of 28 ft/s, with a preferred impact velocity of 8 ft/s, the latter value allowing our canopies to perhaps someday also be used for personnel drops.

We were also constrained by a finite amount of available canopy fabric. As we used the same fabric types in the construction of both competing canopy designs, we had to ration our fabric supply carefully. Furthermore, for manageability during construction and testing, the size of both canopies had to be kept within reason. We aimed for a post-transformation canopy diameter of no more than five feet, which would allow for realistic assembly times and easy drop-testing from high campus windows.

Furthermore, as we were designing our parachutes, we realized that the large post-transformation fabric panels would require careful storage during the pre-transformation flight stage. This forced us to design our post-transformation canopies to be maximally efficient with as little fabric required as possible, as stored fabric can detrimentally affect the gliding performance of the pre-transformation phase. Ultimately, as expected, these constraints led to many compromises between the pre- and post-transformation phases of our design, the details of which will be discussed later.

Design process

In 1919, the McCook Flying Field parachute development team established design guidelines for early parachutes.[3] While times and parachutes have since changed, many of those guidelines are still followed today. First, it was decreed that a parachute's operation should be relatively simple, and that it should not be susceptible to damage from ordinary service conditions. Second, a parachute must be able to withstand opening shocks and slow its cargo down to a predetermined velocity, while at the same time being steerable. The force it transmits to its cargo should be kept to a minimum, and it must be easy to rig and maintain.

In more recent years, parachute engineer Theo Knacke has restated these guidelines in terms of technical design parameters. According to him, a well-designed cargo parachute should be reliable, stable, and have the following characteristics: high drag, low weight and volume, repeatability of performance, adaptability, and low cost.[2] Taking these parameters and our own constraints into consideration, we spent five weeks inventing and developing twelve possible parachute transformation concepts, as illustrated below.

Fabric storage concepts: designs #1, #2, #3 and #4

These concepts, illustrated in Fig. 5, were considered only as early two-dimensional possibilities for how spare pre-transformation fabric could be stored. Design #1 seemed

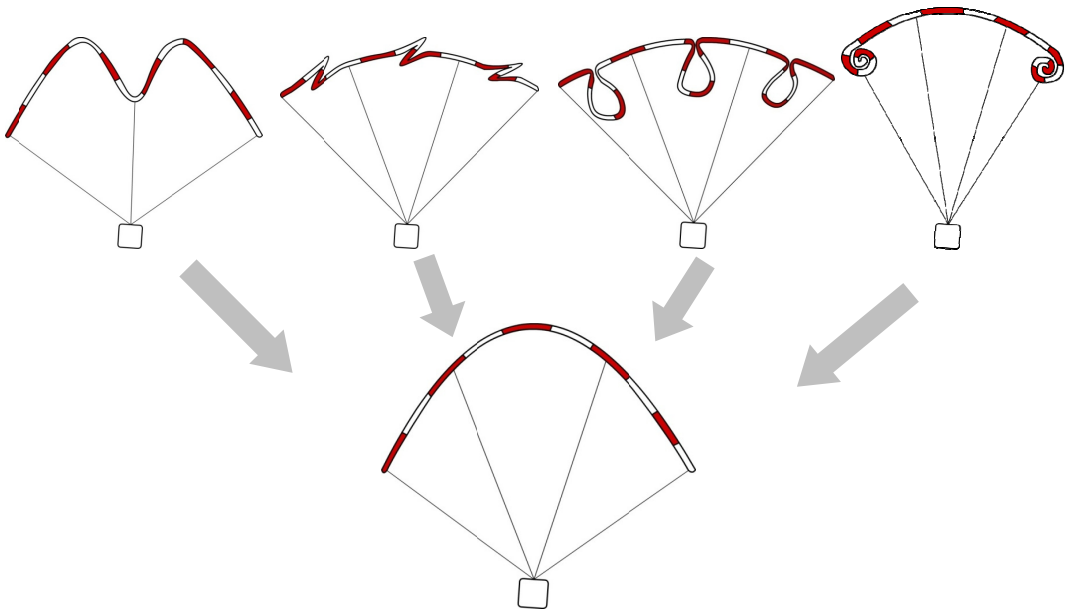

Figure 5: Designs #1, #2, #3 and #4

reasonable at first, but its practicality was quickly called into question. Design #2 was soon dismissed for the un-aerodynamic way the spare fabric was being stored – efficient gliding requires one or more smooth airfoil surfaces, and none were present in Design #2. Design #3's storage method was not very different from Designs #1 and #2, and would also have been un-aerodynamic.

Design #4, however, combined the ability to unroll stored fabric, even against oncoming air movement, with a compact and smooth, aerodynamically satisfactory profile. We selected it as our final method for storing the fabric needed post-transformation.

Rotating concepts: designs #5 and #6

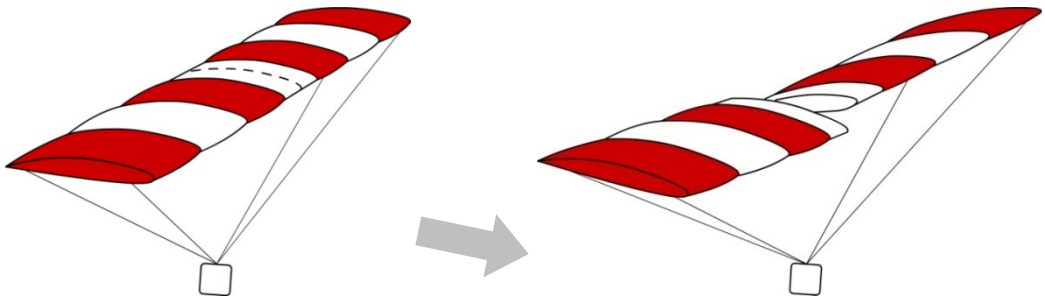

Figure 6: Design #5

Design #5 was the first fully developed design concept that received serious thought and consideration. Both Designs #5 and #6 take their inspiration from nature, which has evolved gentle-descent solutions like the maple seed. Both designs would glide as an airfoil prior to transformation, then descend to the ground while rotating. While these are elegant and perhaps even ideal on a very small scale, their usefulness to clients like the U.S. Army, which could be dropping vehicles and other large payloads unsuited to significant rotation, is limited. Furthermore, because Design #5 integrates what amounts to a hang-glider wing prior to transformation, it would require some sort of solid structural frame, and this project's goal is to design a completely non-rigid, fully collapsible parachute. As such, Design #5 was dismissed.

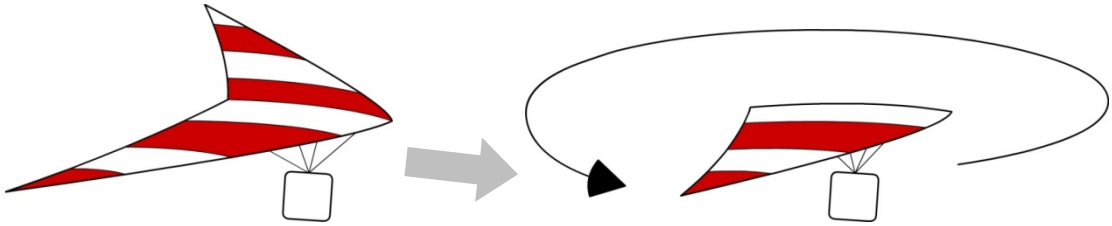

Figure 7: Design #6

Design #6 is the second of our two rotating design concepts. Again, it is an emulation of the principle behind the maple seed, but it has the same shortcomings as Design #5, including the need for a rigid structure. Furthermore, after the design has transformed and one half of the airfoil has been jettisoned, what becomes of the liberated half-wing, and how does this affect the design's reusability? Our inability to answer these questions satisfactorily ultimately led us to dismiss this design.

Transformation concept: design #7

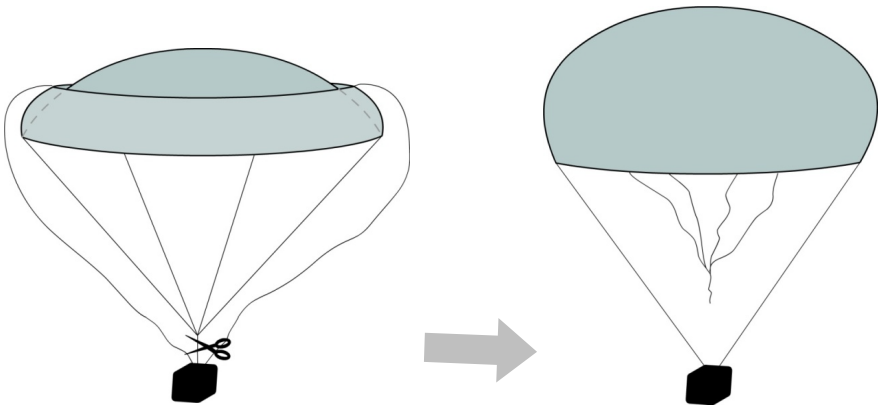

Figure 8: Design #7

Design #7 was more conceptual than practical. It served as an illustration of one way dynamic air pressure could be used to power the transformation, permitting a single, small action near the payload (slackening canopy lines) to cause a major canopy shape change. While not implemented exactly as depicted in Fig. 8, the same principle was expanded upon and ultimately applied in our final prototypes.

Parafoil concepts: designs #8, #9, #10 and #11

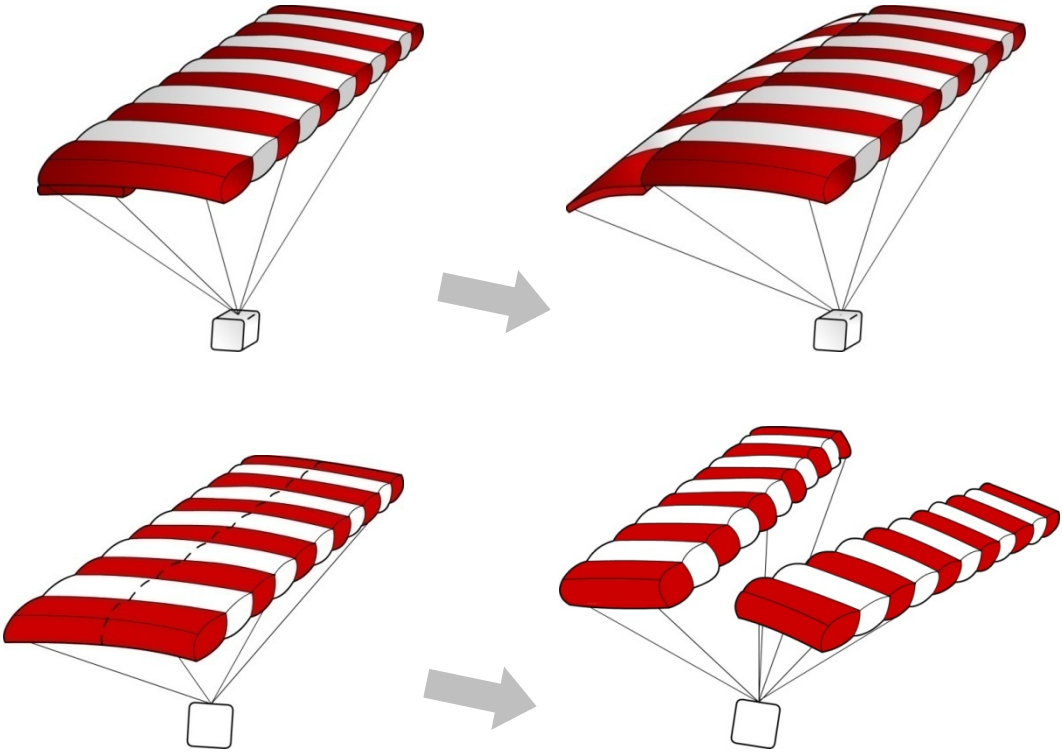

Figure 9: Designs #8 (top) and #9 (bottom)

Design #8 is parafoil-based transformation concept, emulating the principles behind flaps on conventional fixed-wing aircraft. It was dismissed in favor of more comprehensive designs, especially given that flaps can act to slow but not entirely stop the forward motion of a parachute. In Design #9, a single gliding parafoil splits in two to vent air and reduce its forward velocity. However, Design #9 was unanimously determined by sponsor and team alike to be "half-baked." That is, it may have made sense at some basic level on paper, but has no grounding whatsoever in reality. Besides the aerodynamic difficulties of effecting a transformation in this manner, there would be a significant technological hurdle in actually causing a parafoil to split neatly down the middle at the desired time.

Design #10 was another parafoil-derived design concept. Simplicity was its primary advantage, given that it didn't transform so much as *de*form. The design would steer itself to its designated target with tugs to the trailing edges, and then enter a steep vertical descent spiral as it neared the target. This design's major shortcoming is that, while it was

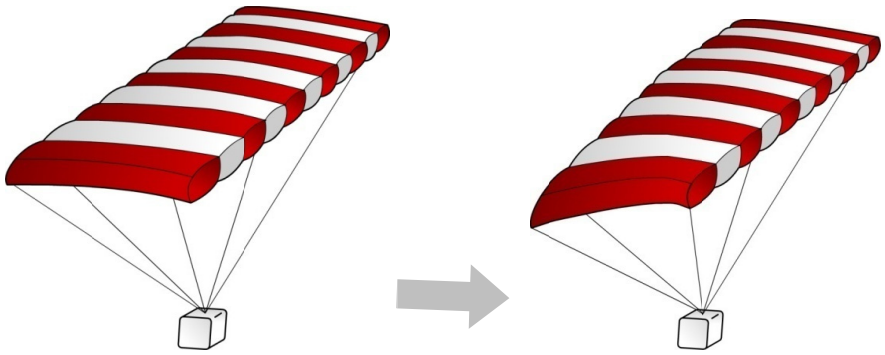

Figure 10: Design #10

invented independently, it operates in exactly the same manner as MMIST's "Sherpa," a commercially available, GPS-guided, parafoil-based cargo delivery system.

Design #11, shown in Fig. 11, is a parafoil-style parachute that unrolls fabric stored around its edges to become a round parachute. As the vertical walls inflate during transformation, the channels on the top would collapse as the forward velocity of the canopy decreases. This design was one of two selected by our sponsor as a final design concept for both its simplicity of rigging and its minimal forward velocity after transformation.

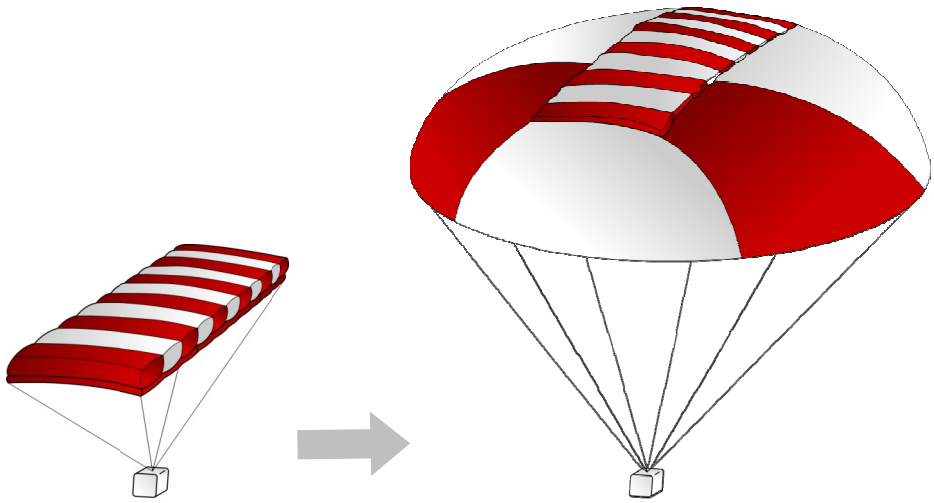

Figure 11: Design #11, ultimately selected as one of our two final designs

Sailwing concept: design #12

Another final design, the second selected by our sponsor for further development, transforms from a Barish sailwing into a cross parachute. As with Design #11, Design #12 integrates two tried-and-tested parachute canopies, the sailwing and the cross parachute. Unlike Design #11, however, which incorporates a large skirt of fabric around the outer perimeter of the parafoil, Design #12, shown in Fig. 12, transforms by unrolling two arms of the cross parachute from beneath the sailwing airfoil (as illustrated in Design #4).

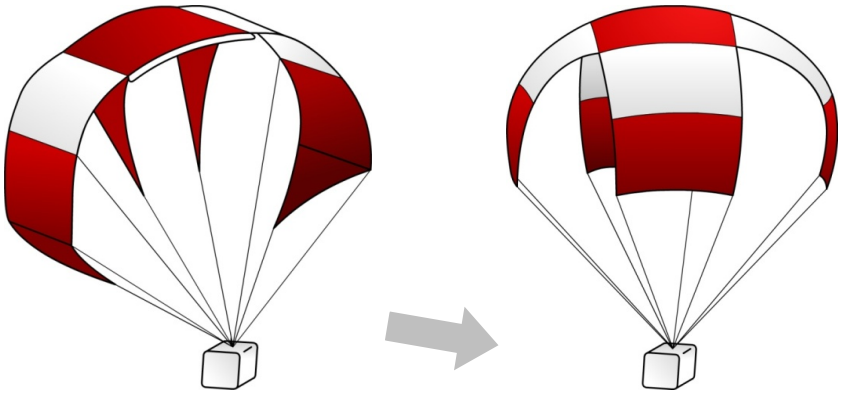

Figure 12: Design #12, ultimately selected as the other of our two final designs

Final design selection

Early in the design process, we decided to pursue two concurrent design routes, one involving a single-surface design (the sailwing) and the other based on a dual-surface parafoil. Doing so would permit us to compare and contrast the canopies' performance and other criteria. From the above designs, our sponsor ultimately selected Designs #11 and #12 for detailed development. The following sections delve into more detail about each design.

Design #11: parafoil to round parachute

Design #11 consists of a parafoil pre-transformation, and a round parachute post-transformation. The pre-transformation canopy, hereafter referred to as the "parafoil," was made from a non-porous rip-stop nylon typically used in personnel ram-air parachutes, while the post-transformation canopy, hereafter referred to as the "round parachute," was made of a *porous* rip-stop nylon typically used in medium weight (5,000- to 10,000-pound payload) cargo parachutes.

The parafoil was designed such that a payload weight of five pounds would descend with a vertical velocity component of no more than 8 ft/s. Using a parafoil lift coefficient[12] (C_L) of 0.435, a drag coefficient[12] (C_D) of 0.15, an air density[13] (ρ) of 1.247 kg/m^3, and the following equations, we find that the total fabric area of the parafoil should be 1.34 m^2.

$$\text{Resultant force coefficient} = C_r = \sqrt{C_L^2 + C_D^2} \qquad \text{Eq. 1}$$

$$\text{Total fabric surface area} = S_o = \frac{2W}{V_t{}^2 \rho C_r} \qquad \text{Eq. 2}$$

From literature[12], we know that parafoils typically have a ratio of top to total fabric surface areas of $\frac{S_w}{S_o} = 0.27$, so our parafoil has $S_w = 0.3618$ m^2. Assuming a historically based parafoil aspect ratio of 3/2, we can calculate the size of all pieces of our parafoil. For simplicity in calculation and construction, we decided to use rectangular pockets (all cross-sections). The labeling scheme of the parafoil can be seen in Fig. 13. Knowing that $AR = \frac{b^2}{S_w}$

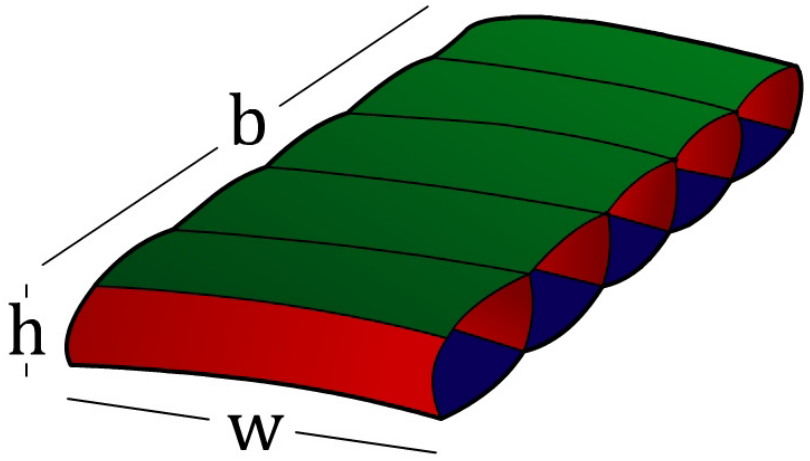

Figure 13: Parafoil dimension variables. Green is the upper surface (area = S_w), blue is the lower surface, (assumed to be equal in area to the upper surface = S_w), and red is the panels, including the outside edge panels.

= 3/2, we can find that b = 0.74 m, w = 0.49 m, and h = 0.21 m. We decided to build our parafoil with five pockets, so a total of six red panels were needed.

To dimension the post-transformation round parachute, the equations[14] below were used, with a drag coefficient[15] (C_D) of 0.75, intended descent velocity (V) of 8 ft/s and air density (ρ) of 1.247 kg/m^2. Payload weight (W) was reduced to 1 lb due to limitations on the amount of fabric available; this compromise is discussed later.

$$\text{Total round parachute surface area} = S_o = \frac{2W}{V^2 \rho C_D} \qquad \text{Eq. 3}$$

$$\text{Round parachute diameter} = d = 2\sqrt{\frac{S_o}{\pi}} \qquad \text{Eq. 4}$$

The total area of the round parachute was therefore calculated to be 1.6 m^2, with a nominal diameter (d) of 1.43 m. The Appendix contains the pattern used to create one quarter of the round parachute; it was used four times to construct and assemble the finished transforming canopy as illustrated in Fig. 14. Final dimensions were found using simple proportions and trigonometry.

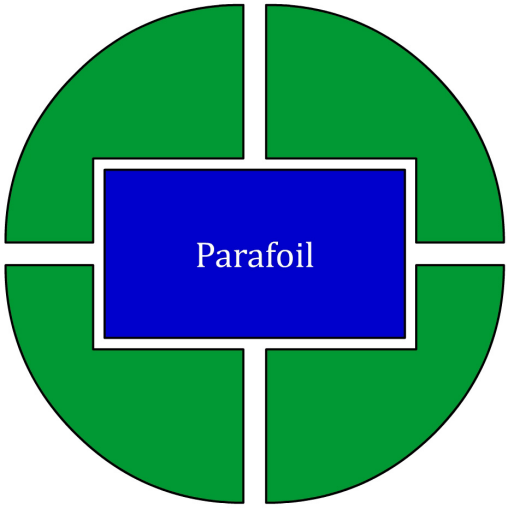

Figure 14: Diagram of assembly for four panels of round parachute and already assembled parafoil

As mentioned above, the requirement for a very large post-transformation canopy compared to the relatively small pre-transformation parafoil led to the pre- and post-transformation canopies actually being designed for *different* payload weights. In reality,

the payload weight cannot be changed mid-flight, and so the total weight our parachute could carry was in fact limited by the size of the post-transformation canopy.

Design #12: sailwing to cross parachute

David Theodore Barish (b. 1921) was a pilot for TWA and later became a theoretical aerodynamicist employed by the U.S. Air Force and NASA. He contributed more than just the sailwing to parachuting; he invented the "vortex ring" in 1955, a design still in use today.[18] Developed in the mid-1960s, Barish's "sailwing," as it came to be known, was a single-surface contemporary to Domina Jalbert's parafoil. The first incarnation had three lobes, and its leading edge was folded under for 30 cm and stitched down to add a degree of rigidity. A five-lobed version was introduced in 1966, with the folded-under portion extended to one third of the total chord. Early versions used spinnaker cloth from sailmakers for the lowest possible porosity when gliding.[18] All of Barish's designs have characteristic vertical stabilizing fins descending from the main canopy.

At the time of its introduction, the sailwing had several advantages over contemporary parachute technology. It was a single-surface canopy, and was, therefore, simple to manufacture and used less fabric. It had much less bulk and surface area than a round parachute, but its descent rate was half; it converted vertical drag into forward velocity and was an apt glider. Perhaps most importantly, it allowed jumpers to land accurately on a target, even on their first jumps with the canopy. Furthermore, its opening shock was "comparable to low porosity, flat circular canopies," a desirable attribute indeed.[19]

Figure 15: Francis Heilmann's 1965 Barish sailwing model on display at the 2005 Icarus Cup in France.[17]

The Air Force officially measured a maximum in-wind tunnel L/D ratio of 4.2 for the sailwing,

although in practice the number is lower. Sailwing aspect ratios have ranged from 3 for skydiving to 5 for slope-soaring.[20] Other reported specifications include a sink rate of 3 m/s and a forward speed of around 20 mph (these correspond to a more reasonable L/D of around 2.5).[21]

Forty years after its invention, the sailwing was "reintroduced" in 2005 at the 32nd annual Icarus Cup in Lumbin, France, shown in Fig. 15. Discovering that there were no extant plans for the sailwing, parachutist and builder Francis Heilmann based his model solely on two historical photos. His design had a surface area of 40 m^2, a wingspan of 13 m, 5 lobes, and semi-rigid keels to maintain the wing profile. David Barish himself was present at the unveiling, and Heilmann's parafoil performed admirably during its first flight on July 13, 2005.[22]

We encountered the same difficulties Francis Heilmann did while designing our sailwing. Specifically, due to its inferiority to the parafoil and its resulting rarity forty years after its introduction, there is not a lot of information available to those who wish to build a sailwing today. Like Heilmann, then, we based our design largely on photographs, most of Heilmann's own sailwing. In doing so, we risked propagating any errors Heilmann may have made, but given his experience with parachutes and that his design did fly, we accepted the risk.

Fortunately, we also found a valuable resource that Heilmann did not, in the form of NASA reports. In the late 1960s, NASA conducted "wind-tunnel tests of a series of parachutes designed for controllable gliding flight"[23], a "wind-tunnel investigation of the static aerodynamic characteristics of a multilobe gliding parachute"[24], and a study of "gliding parachutes for land recovery of space vehicles"[25]. Each of these involved the sailwing, and all provide drawings and quantified performance characteristics.

The most useful report was the one that tested "a series of parachutes," because it

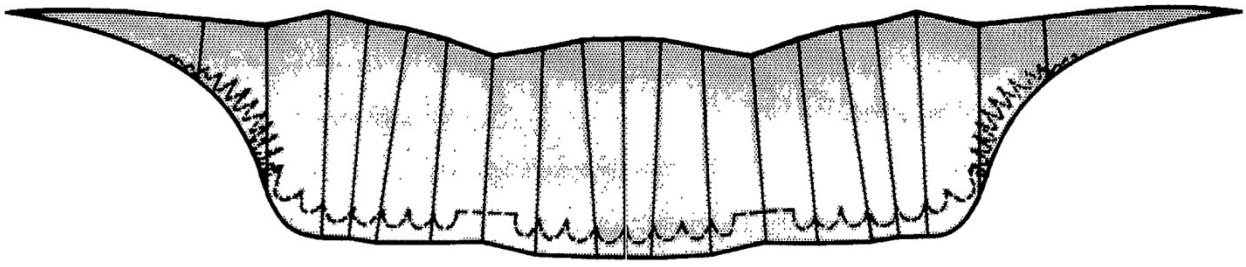

Figure 16: Three-lobed sailwing design from the NASA-TN-D-3960 report.[23]

compared three different sailwing designs. Two had five lobes, and the third had three lobes. At the cost of performance, we chose to build the three-lobed design, to simplify construction and rigging, and to help avoid tangling during testing.

The "series of parachutes" report conveniently provided flat plans for each sailwing design. NASA's plan for the three-lobed sailwing is reproduced in Fig. 16. In this drawing, the trailing edge is up; the dotted line pattern along the bottom edge indicates that extra material is folded over and secured to provide rigidity to the leading edge. We chose not to include this material in our design, to avoid interference with the post-transformation fabric. This decision likely had an adverse effect on our sailwing's performance, but was a necessary sacrifice in light of more important design goals.

We sized our sailwing using a standard formula for gliding parachutes[2]:

$$V_t = \sqrt{\frac{2W}{S_o \rho} \cdot \frac{1}{C_r}} \qquad \text{Eq. 5}$$

where V_t is the trajectory velocity, W is the total system weight, S_o is the total fabric surface area, ρ is the air density, and C_r is the lift-drag resultant force coefficient.

It was found in the NASA reports that the sailwing requires an angle of attack (α) greater than 22° to stay inflated, and that it generates the most lift at that angle. We selected α = 30° as a safe flight condition away from leading edge collapse, and found, from tables in the NASA-TN-D-4672 report[24], that such an α corresponds to $C_D = 0.55$ and $C_L = 0.95$. With the following formula from Knacke,

$$C_r = \sqrt{{C_d}^2 + {C_l}^2} \qquad \text{Eq. 6}$$

the sailwing's resultant force coefficient, C_r, is 1.097.

At α = 30°, the same table indicates that the sailwing has an L/D of almost exactly 2.0 (substantially worse than an equivalent parafoil, but acceptable for our purposes). If we use our sponsor's design specification of 8 ft/s in vertical descent, this L/D corresponds to a forward velocity of 16 ft/s and a trajectory velocity, V_t, of

$$V_t = \sqrt{16^2 + 8^2} = 17.88 \text{ ft/s} = 5.44 \text{ m/s}\,. \qquad \text{Eq. 7}$$

Now, using Knacke's formula for gliding parachutes and a payload mass of 2 lb (8.89 N),

$$5.44\text{m/s} = \sqrt{\frac{2\ (8.89\text{N})}{S_o(1.247\ \text{kg/m}^3)} \cdot \frac{1}{1.097}} \qquad \text{Eq. 8}$$

one obtains a total surface area, S_o, of 0.439 m^2. The NASA drawing above has an aspect ratio of approximately 3 (not counting the pointed tips), so this surface area corresponds to a prototype sailwing span of 1.15 m and a chord of 0.38 m. Given that our objective called for the sailwing to transform into a cross parachute, two panels were added as shown in Fig. 17.

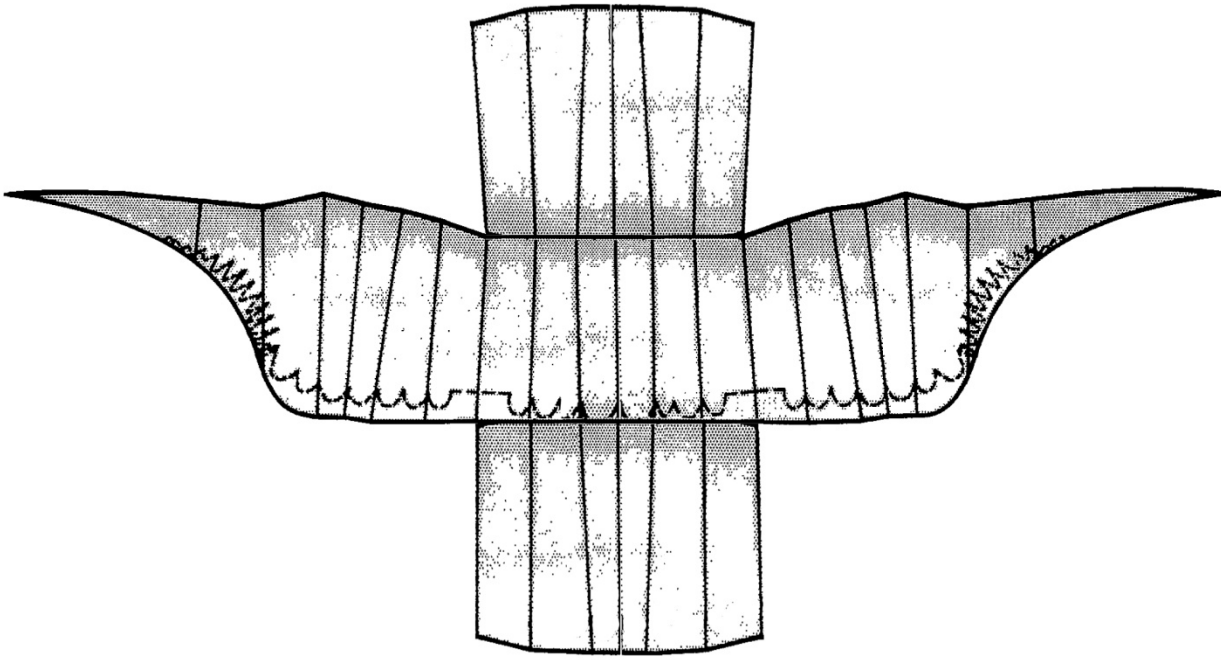

Figure 17: Sailwing with transformation panels added.

These panels were sized so that, when inflated, the bottoms of the four arms of the cross would be at an equal height above the payload, as they are in conventional cross parachutes like the one in Fig. 18. The total area of the cross parachute then became 0.73 m^2, which, according to Knacke's formula,

$$8.89\ \text{N} = \frac{1}{2}(1.247\ \text{kg/m}^3)(\text{V})^2(0.73\ \text{m}^2)(0.6) \qquad \text{Eq. 9}$$

yields a cross parachute descent velocity (V) of 5.7 m/s (18.7 ft/s). As with the parafoil, this post-transformation descent velocity is significantly faster than the 8 ft/s design

specification used in the gliding phase, and again indicates that a compromise in payload weight will have to be reached (i.e., the payload that a sailwing can satisfactorily support is significantly heavier than the post-transformation cross parachute's payload capacity). It also hints at a fundamental problem to be overcome in the design of transforming parachutes: the "equivalent" round (or cross) parachute requires much more fabric than its gliding counterpart, and the storage of this fabric somewhere in the gliding canopy will invariably have an adverse effect on the canopy's performance.

Figure 18: Prototype cross parachute constructed for wind tunnel testing

Once sailwing design and sizing was complete, the pattern shown in Fig. 17 was split into pieces, printed on sheets of 8.5" x 11" office paper, and assembled to form a 1:1 scale version of the sailwing out of paper. This pattern was then cut up into large pieces that would be used to trace the design onto parachute fabric. Figure 19 indicates how the design was divided for individual fabric panel assembly. The two additional pointed blue pieces are vertical stabilizers that attach to the main surface between the lobes. The two colors show the different materials used; the main sailwing and stabilizers are made of blue non-porous rip-stop nylon parafoil fabric, while the cross parachute panels are made of green non-porous round parachute material.

Vertical descent canopies, like round parachutes, typically employ porous fabric, as did ours in Design #11, to avoid oscillation during descent; air trapped under the canopy is able to leak through the fabric rather than escaping uncontrollably from alternating sides of the parachute. However, in the cross parachute, a phenomenon known as "geometric porosity" exists, whereby air can escape from under the canopy through the large holes between arms (clearly visible in Fig. 18). As such, we specified non-porous fabric in the post-transformation phase of Design #12.

The primary reason for using a different-colored material for post-transformation was that there was a shortage of blue fabric at the time of construction, but the different

color also provided a visual indication, from the ground, that the parachute has successfully transformed. Both canopies' panels were individually hemmed (once with a straight stitch and then with a zig-zag reinforcement stitch), then sewn together with the same stitching procedure.

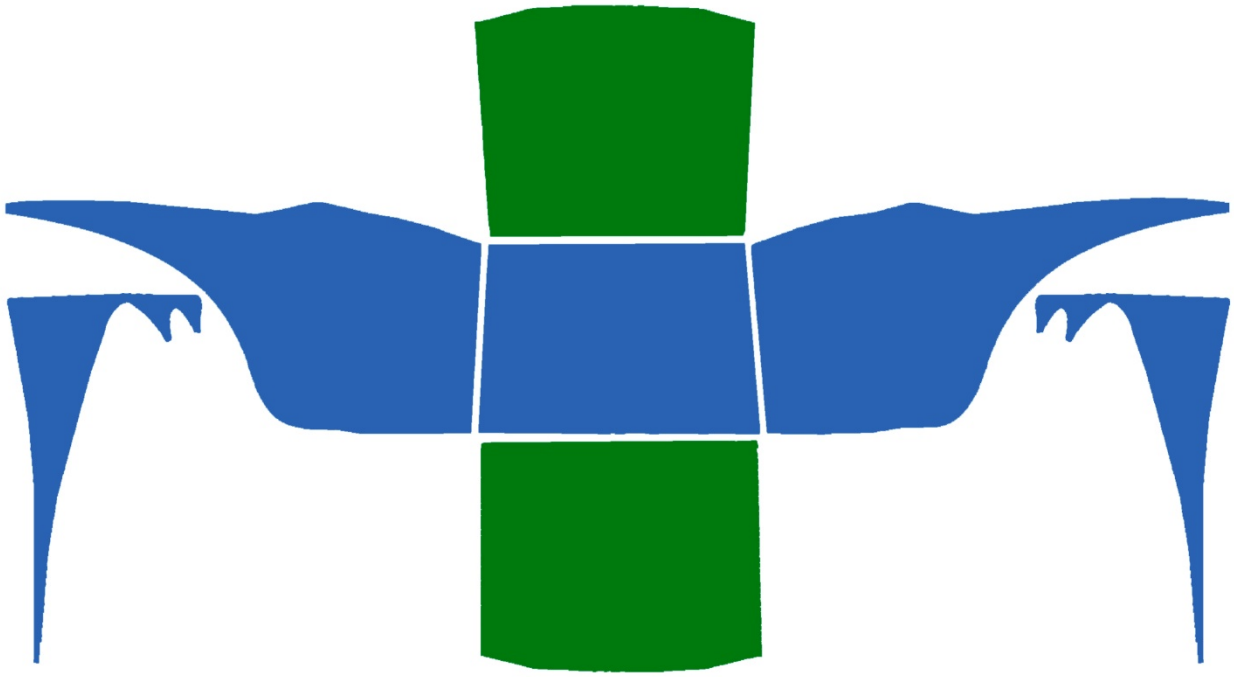

Figure 19: Fabric pattern for sailwing/cross parachute.

Parachute descent theory

The "parachute problem" ordinary differential equation (ODE) is a favorite of mathematicians and physicists, and it has been studied in great detail. Some have applied computational tools like Maple to help solve the problem.[27] An outline of the basic theory and some results follow.

When their descent profiles are considered fully, our transforming parachutes have three descent modes: free-fall (phase I), glide (phase II), and vertical descent (phase III). Each mode is governed by the same non-linear differential equation,

$$m\ddot{y} = -mg + k\dot{y}^2, \qquad \text{Eq. 10}$$

where m is the total mass of the parachute and payload, g is the acceleration of gravity, k is a constant relating to the force of air resistance ($k = \frac{1}{2}\rho S_o C_D$), and y and its derivatives refer to motion in the vertical axis only.

Using the initial conditions $y(0) = y_0$ and $v(0) = v_0$, exact solutions are easily obtained with a package like Maple. The following lines of code,

```
> with(DEtools):
> dsolve({m*diff(diff(y(t),t),t)+m*g-k*diff(y(t),t)^2=0,y(0)=y0,
D(y)(0)=v0});
```

can be used to find expressions for the parachute's vertical position and descent velocity, respectively:

$$y(t) = \frac{1}{2}\frac{2\sqrt{g}\sqrt{k}\,t\,m^3 + m^{(7/2)}\ln\left(\frac{4\,m^5 k^2 g}{\left(-\mathbf{e}^{\left(\frac{2\sqrt{g}\sqrt{k}\,t}{\sqrt{m}}\right)} k\,m^{(5/2)}\sqrt{g} + \mathbf{e}^{\left(\frac{2\sqrt{g}\sqrt{k}\,t}{\sqrt{m}}\right)} k^{(3/2)} m^2\,v0 - m^{(5/2)}\sqrt{g}\,k - k^{(3/2)} m^2\,vo\right)^2}\right) + 2\,m^{(5/2)}\,k\,y0}{m^{(5/2)}\,k}$$

Eq. 11

$$v(t) = \frac{1}{2}\frac{2\sqrt{g}\sqrt{k}\,m^3 - \frac{2\,m^{(7/2)}\left(-2\,g\,k^{(3/2)} m^2\,\mathbf{e}^{\left(\frac{2\sqrt{g}\sqrt{k}\,t}{\sqrt{m}}\right)} + 2\sqrt{g}\,k^2\,m^{(3/2)}\,\mathbf{e}^{\left(\frac{2\sqrt{g}\sqrt{k}\,t}{\sqrt{m}}\right)} v0\right)}{-\mathbf{e}^{\left(\frac{2\sqrt{g}\sqrt{k}\,t}{\sqrt{m}}\right)} k\,m^{(5/2)}\sqrt{g} + \mathbf{e}^{\left(\frac{2\sqrt{g}\sqrt{k}\,t}{\sqrt{m}}\right)} k^{(3/2)} m^2\,v0 - m^{(5/2)}\sqrt{g}\,k - k^{(3/2)} m^2\,vo}}{m^{(5/2)}\,k}$$

Eq. 12

The constant values in Table I were used to approximate the specifications of our constructed parachute systems when applying the differential equation.

Table I: Constant values used in ODE modeling

mass	m	3 lb = 1.4 kg
gravitational acceleration	g	9.81 m/s^2
air resistance constant (free fall)	k	$\frac{1}{2}\rho S_o C_D = 0.01$
air resistance constant (sailwing, glide)	k	0.26
air resistance constant (parafoil, glide)	k	0.36
air resistance constant (cross parachute)	k	0.25
air resistance constant (round parachute)	k	0.80

Some approximations have been made: the free-falling, unopened parachute is approximated as a smooth sphere 30 centimeters in diameter, and all drag coefficients are based on historical literature, not our own experimentation (except the cross parachute's, which we measured during wind tunnel experiments, as discussed later).

The solutions to this ODE can be used to determine a number of properties of our parachute systems. One can easily find the theoretical terminal velocities for each mode by examining the value of $v(t)$ as $t \to \infty$, yielding the values in Table II.

Table II: Theoretical canopy terminal velocities

Free fall	35.7 m/s	=	80 mph
Sailwing glide	7.0 m/s	=	16 mph
Parafoil glide	5.9 m/s	=	13 mph
Cross parachute	7.1 m/s	=	16 mph
Round parachute	4.0 m/s	=	9 mph

The discrepancy between these values and the original design constraint of 8 ft/s (2.4 m/s) is a reflection of the many compromises we had to make during our design. For instance, a shortage of parachute material and the desire for more manageable sizes led us to build smaller canopies than originally planned, while the minimum payload weight (servos, etc.) could not be reduced beyond a certain point. Another compromise, discussed in more detail in the design section, was to balance gliding performance with the storage of large amounts of material to be used post-transformation.

Obviously, discontinuities in the ODE results exist when a parachute transforms from one mode to another. These can be easily reconciled by setting the new mode's initial conditions at the time of transformation to the old mode's final values at that same time. With the above theory in place, we can examine our systems' expected behavior using some roughly real-world conditions.

In particular, we have examined the case of our final drop test from a helicopter. While actually dropped from around 300 feet above ground level (AGL), the initial plan was to use an altitude of 400 ft. AGL, and we assumed here, based on our own drop test observations, that the system spends two seconds in freefall from this altitude before the

gliding canopy deploys. Working backwards from landing, we can also find the minimum time and distance before landing that each system must spend in its final vertical descent mode to reach an acceptable impact velocity (i.e., within 0.1% of its terminal velocity), if its initial velocity is the terminal velocity of the previous (i.e., gliding) mode. This is shown in Table III.

Table III: Minimum time and distance needed in post-transformation mode to reach acceptable impact velocity

	Time	Distance
Cross parachute	1.09 seconds	7.8 feet AGL
Round parachute	1.21 seconds	4.8 feet AGL

After 2 seconds of freefall from 400 feet AGL, both systems will have a descent velocity of 17.86 m/s and will be 338 feet AGL. Assuming transformations occur instantaneously, we can find the time until the system descends to 100 feet AGL, at which point we planned to trigger the transformation to the vertical descent mode. While the values indicated above correspond to the theoretical "last possible instant" to trigger an instantaneous transformation to the final descent mode, real-world inflation times and the desire to observe the system in both modes would indicate that transforming earlier, i.e., around 100 feet AGL, would be a good idea, as long as winds were light (to prevent sideways drift).

The first two lines of Table IV contain the times each gliding canopy must spend in gliding mode before transforming to vertical descent mode. Finally, with the conditions and time of transformation known, it is a simple matter to determine the time after deployment at which each system will theoretically touch down in its vertical descent mode. These times are shown on the second two lines of Table IV.

Table IV: Glide times for each mode

Sailwing	t = 11.9 seconds
Parafoil	t = 13. 8 seconds
Cross parachute	t = 16.2 seconds
Round parachute	t = 21.3 seconds

All of the above results are summarized in the plot of descent velocity in Fig. 20.

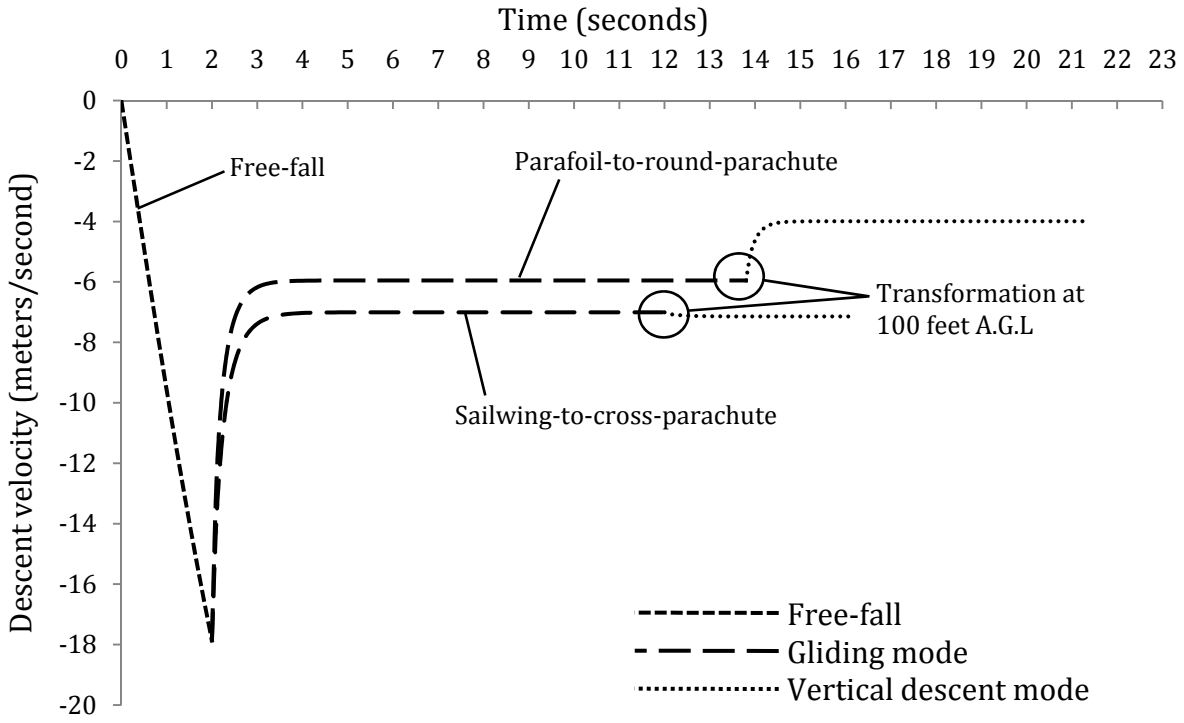

Figure 20: Plot of predicted canopy descent velocities over time for drop from 400 ft. AGL

One notices that the parafoil/round parachute system has a lower predicted impact velocity, and that there is a more significant difference in its descent velocity pre/post-transformation. The sailwing/cross parachute system's descent velocity actually *increases* slightly after transformation, an undesirable condition resulting from the cross parachute's relative poor performance as a decelerator, when compared to the round parachute.

Further insight can be gained by examining the systems' motion in two dimensions. The following two additional assumptions are made:

- The system is thrown clear of the helicopter horizontally at 10 m/s.
- In the glide phase, the system's horizontal velocity is correlated to its vertical velocity using the designs' L/D values.

The same differential equation (with the effects of gravity removed) can be used to determine how the systems' horizontal motion decays during free-fall and vertical descent modes as a result of air resistance. Results are plotted in Fig. 21.

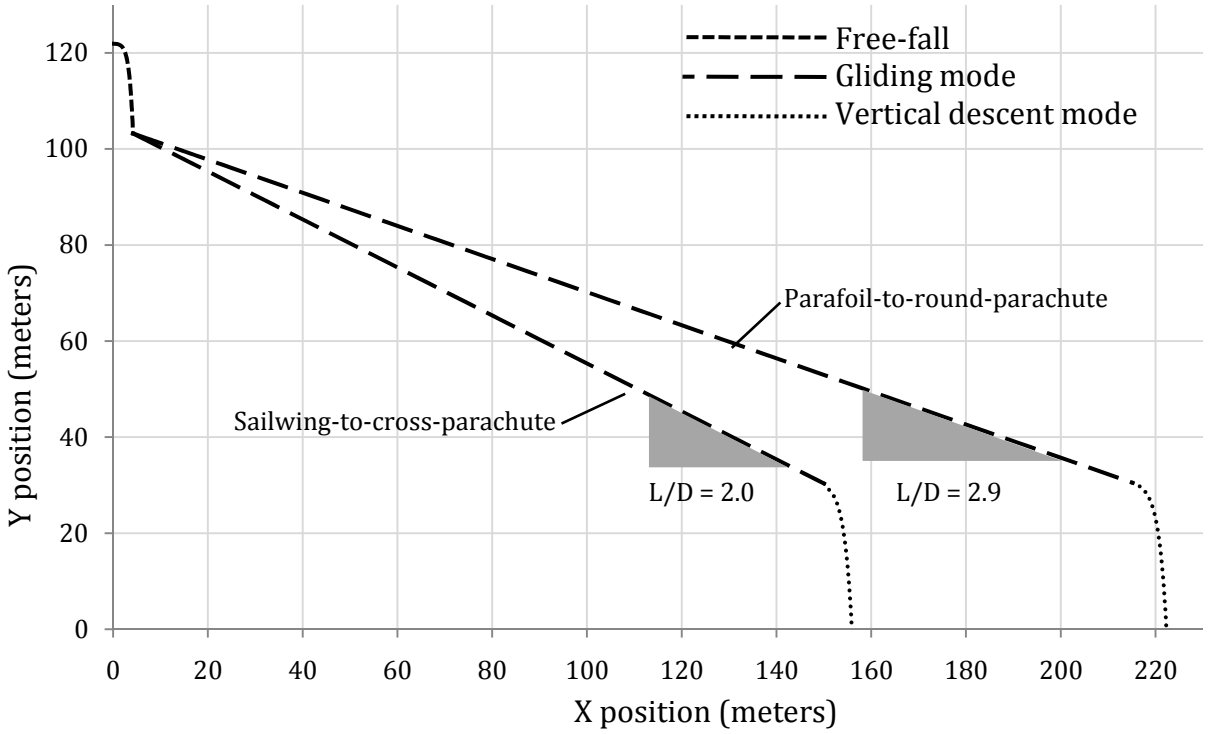

Figure 21: Plot of predicted canopy descent trajectories for drop from 400 ft. AGL

It is evident that, for a given drop altitude, the parafoil/round parachute system is predicted to achieve a greater offset (in fact, 43% greater) than the sailwing/cross parachute system. This is due to the parafoil's higher L/D ratio.

Transformation system and techniques

When designing the system that would facilitate the transformation of our parachutes, there were several issues that had to be considered for each parachute and system. Our challenge was to select solutions that would provide an optimal balance between performance and reliability. To that end, we spent a significant amount of time researching methods being used in similar applications, inventing new methods of our

own, and testing different ideas and materials on a sacrificial prototype cross parachute canopy constructed early in the project for wind tunnel testing.

The first issue considered was that of fabric storage prior to transformation. The method of fabric storage could have a detrimental effect on the aerodynamic properties of the gliding canopies, including their L/D ratios. Consequently, we had to ensure that the method we chose did not adversely affect important flight properties. However, making sure the fabric was safely secured was just as important. To satisfy our project objective, each parachute must maintain its initial shape until the moment of transformation. Any premature compromise of canopy shape could drastically change the flight properties of the pre-transformation stage, unintentionally modifying flight paths and descent rates, or even causing catastrophic failure or system loss. In short, it was very important that our chosen method of fabric storage be both secure and stable during flight.

Another issue we considered for each system was the rigging of the parachute lines. Rigging had to be both simple and reliable. Complex rigging does not permit easy packing of parachutes, and is more prone to packing mistakes and deployment failures. Therefore, in order to assure reliability of operation, our rigging system had to be uncomplicated and able to deploy and control the parachute canopies reliably and consistently.

Finally, we considered how to actually trigger the transformation. This issue was perhaps the most flexible, with many different methods and materials to choose from. Whatever the method chosen, it had to be compatible with the fabric storage and rigging methods we selected in order to be effective. Much like rigging, a simple transformation mechanism would allow for easier packing and a better likelihood of proper and reliable operation. Like with fabric storage, it was important that the transformation mechanism operate only at the right time. Premature, late or partial transformation could once again result in the parachute landing off-target, an undesired decent rate, or even a total loss of the system. Therefore, the transformation mechanism had to be precisely and reliably controllable. The system we ultimately selected to trigger the transformation adhered to these requirements, ensuring the greatest probability of success of all options considered.

Systems for the storage and securing of fabric

There were two main factors considered after systems for the storage and securing of fabric for the post-transformation stage were chosen. These were in the areas of aerodynamic properties and stability. Each was important to our canopies, and of course we desired the best mixture of these two attributes. Any method of storing fabric needed to be entirely contained beneath the canopy of the parachute – storing fabric on the top of the parachute would have adversely affected the parachute's aerodynamic gliding properties.

One option for storing fabric was folding. The folding of extra fabric gave a low profile that, satisfactorily, did not affect aerodynamic properties to any appreciable degree. However, rip-stop nylon fabric was not conducive to folding. When folded, the fabric had a tendency to unfurl, and not always in the desired direction. In order to have made folding a viable option, the folded fabric would have needed to be properly secured in combination with other complicated methods.

Another option for storing fabric was rolling. Rolling did not provide as low a profile as folding. However, if done correctly, we discovered that rolling can provide a curved edge, much like a crude airfoil, that could possibly enhance L/D ratios and other aerodynamic properties. While rolled fabric also required securing prior to transformation, it was not as unstable as folding, and it almost always unfurled in the desired direction, even against oncoming airflow.

Stored fabric had to be properly secured so that the transformation could be controlled and triggered at the correct moment. One proposed method of doing this was to use Velcro. Velcro offered a good balance between security and ease of release. However, in order to trigger the transformation with Velcro as the securing component, some sort of pulling force would be required. Similarly, though not as optimal and without the textile flexibility of Velcro, snaps and adhesives could have been used along the same lines.

Fabric securing could also have been done with knots or some form of temporary stitching. This would have also required a pulling force from the transformation mechanism, and re-rigging would have been complicated.

Another scheme, the one we ultimately selected, employed conventional iron magnets. While not ideal for full-size canopies because of safety and deployment issues

associated with large magnets in aircraft, our small craft magnets allowed for easy testing and deployment on our scale models.

One method, differing from the others mentioned previously, would have been to secure fabric with rigging loops. In this system, extra fabric would have been rolled underneath the parachute. Rigging would have followed on the outside surface of the parachute and would have gone through small holes on the top of the canopies. In this way, when the rigging was in tension (e.g., from the payload during flight), it would secure the post-transformation fabric. In order to trigger the transformation, rigging slack would simply need to be released using one of the following transformation mechanisms. However, this method requires a complicated rigging system, undesirable in our implementation.

After some preliminary testing, we selected a combination of rolled fabric and conventional magnets to store and secure our pre-transformation fabric in both canopies. Magnets were chosen for their ease of use and reliability of release when significant force was applied. The rolling method was selected because of the possible beneficial effects on aerodynamic properties, satisfactory stability in pre-transformation mode, and reliability to unfurl correctly every time.

Transformation mechanisms

During our design process, many ideas for transformation mechanisms were suggested, and many discarded. Below are ideas that were seriously considered for implementation on the transforming canopies.

Bead/knot method

This is a method of releasing slack, as shown in Fig. 22. The line slack is held in place by an obstruction, such as a bead or a knot. Once the servo disk rotates, the obstruction is permitted to pass through. The line slips through the hole in the disc, releasing slack until it is stopped by a second obstruction below the servo. This allows for precise control of how much slack is released. This system is fully reusable and repeatable, an asset we identified during our testing phase.

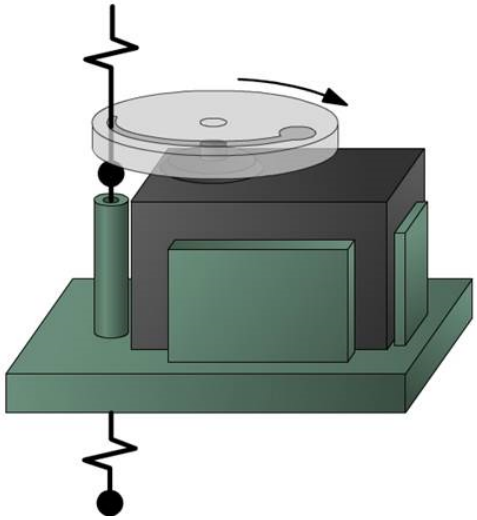

Figure 22: Bead/knot transformation mechanism

Cutting method

This is also a method for releasing slack, shown in Fig. 23. There were, in fact, two possible implementations for this method. In the first scenario, a set of rigging strings are taut and a second set are slack and not in use initially. The taut set is cut by the servo and the payload is transferred to the slack set of rigging strings. The second possibility for this method involves the slack being coiled and held in place by some sort of sleeve. The sleeve is then cut, and the slack releases.

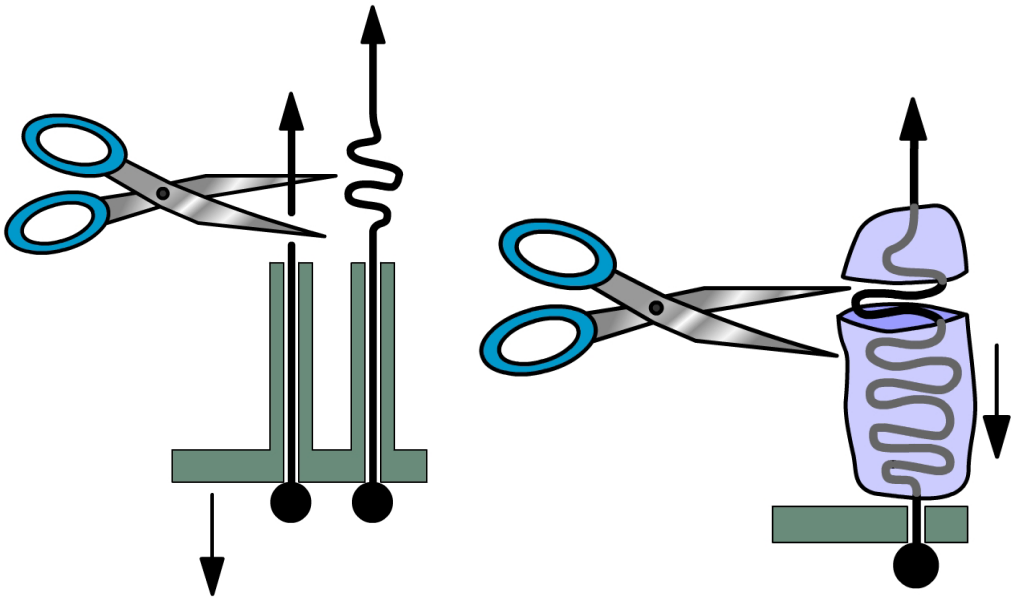

Figure 23: Cutting method; both implementations

Slip knot method

This is another method of releasing slack. In this method, a preset amount of slack rigging is held in place by a slip knot attached to a small loop near the payload. When the servo is activated, it releases or cuts the loop, thereby releasing the slipknot to facilitate transformation.

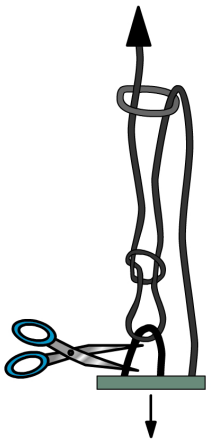

Figure 24: Slip knot method

Drag chute method

This is a method of applying a pulling force to initiate transformation. It would be relatively reusable and we believe it would be a reliable method if done correctly, but only on larger-scale systems. In this method, the servo would release a small parachute in the direction opposite of the gliding canopy's horizontal velocity. This would apply tension on the post-transformation rigging, exerting a pulling force on the stored fabric.

Due to its complexity, however, we never considered this method for our small-scale parachutes.

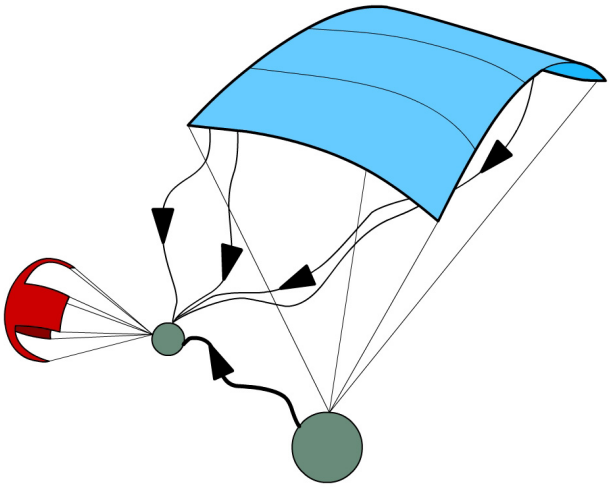

Figure 25: Drag chute method

Winding method

This method could be used to either release slack or provide a pulling force. It involves using an accurately controllable small electric motor. The motor would have a spindle attached to it. Based on transformation requirements, the motor could be run forward to release slack or in reverse to provide a steady pulling force.

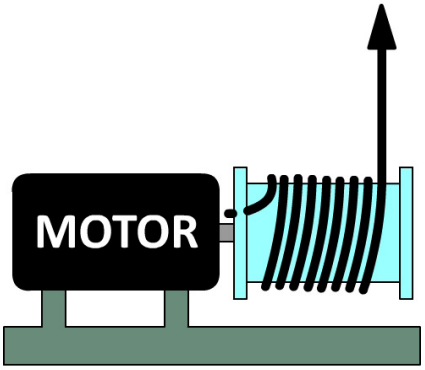

Figure 26: Winding method

In the end, we selected the bead/knot method to initiate transformation. This system was implemented in conjunction with small magnets holding the rolled-up pre-transformation fabric in place. First, pre-transformation lines were held taut by a servo disk, and the pre-transformation fabric was rolled up underneath the canopy; the post transformation lines hang loose at this point. Next, the servo disk is rotated when triggered by remote control. The servo mechanism and payload weight fall, providing the jerking force needed to dislodge the magnets, and the extra fabric unfurls. Finally, the parachute is fully transformed and the pre-transformation lines hang loose. Figure 27 illustrates this sequence of events fully.

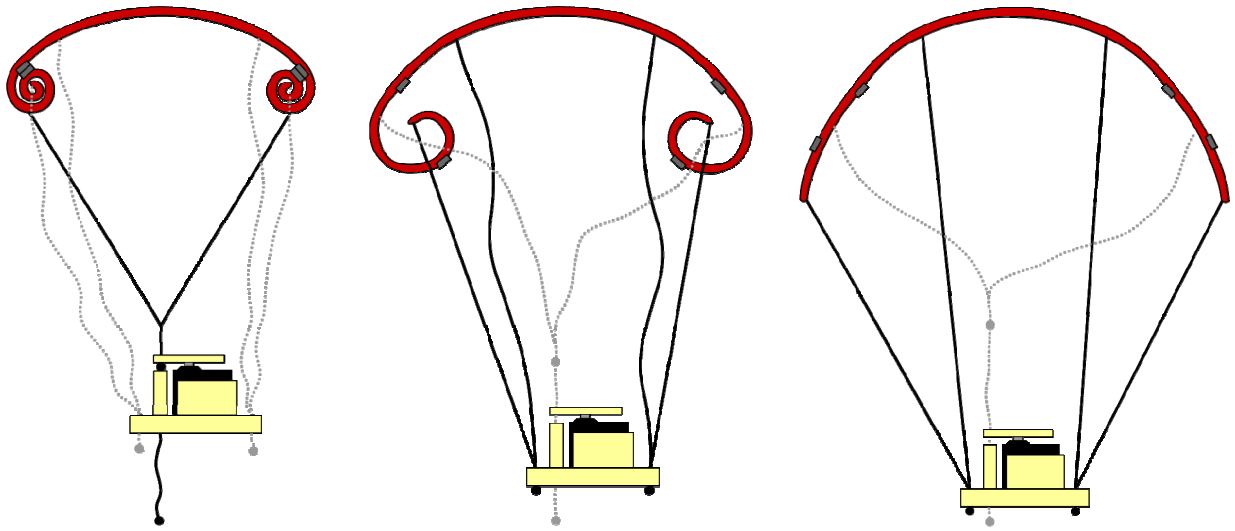

Figure 27: Final transformation concept; three-step schematic of system operation

Rigging systems

The parachutes' rigging systems had to be simple, and they needed to be designed to avoid tangling. As such, rigging was attached to strategic points on the parachute canopies to provide the correct trim when inflated. The simplest rigging system would have been single, continuous lines to these attachment points. However, with the transformation mechanism and two different modes of flight to account for, this was not possible for either prototype parachute.

The selected transformation mechanism design required a set of rigging lines for each stage on each parachute. With the pre-transformation lines held taut to start, two different detangling options were considered. The team tested a slider, which is common in many parachute systems, but was not impressed with its functionality, and, since it could only be used on one set of lines, ultimately decided against its use. Fishing snap swivels were implemented on the final canopies in an attempt to prevent tangling. Swivels had the advantage of low cost, ease of use, and the ability to be installed on all lines.

3D printing

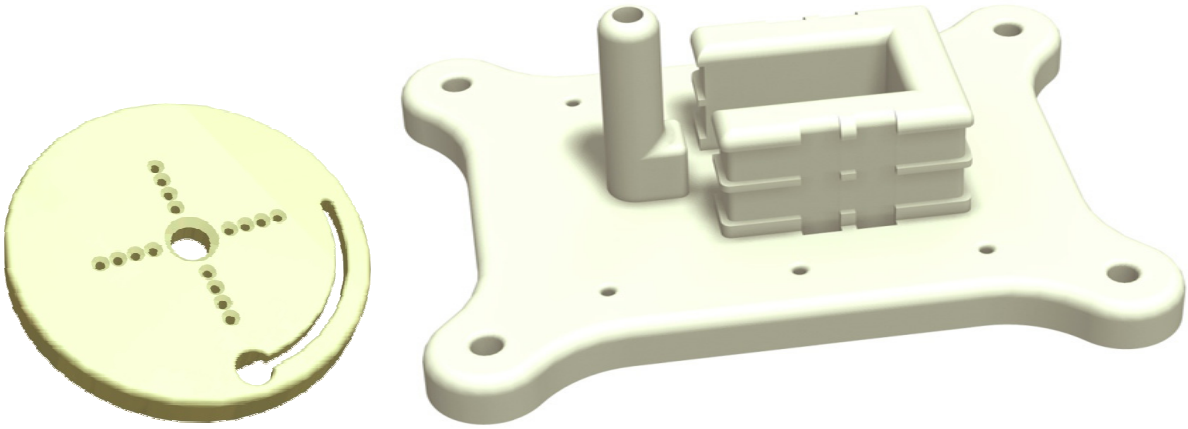

Figure 28: ProEngineer CAD renderings of the 3D-printed components of our transformation mechanism

One technology that allowed the team to fabricate custom parts for the parachute's transformation mechanism was 3D printing. WPI currently owns a Dimension SST 1200es 3D printer, to which we were granted access for this project. This equipment allows the user to produce custom parts of almost any shape and up to a maximum build size of 10" x 10" x 12".[28]

Three-dimensional printing works by taking a .STL CAD file (in our case, created in ProEngineer) and using software to slice the model into segments 0.01" thick; it then builds the part from the bottom up by layering those segments on top of each other in semi-liquid acrylonitrile butadiene styrene (ABS) plastic.[29] If the part being fabricated requires it, a plastic support structure is built first by the machine and then dissolved away once the part has been completed.[28] The machine is network-capable and works in much the same way as a normal printer.[30] Our .STL files were sent over the network to the machine.

We used the machine to build the servo bracket and the servo disk for the bead/knot method. This cost the team a total of $16.64 per set. The enormous savings in time and money over machining complicated parts from aluminum are testaments to the usefulness of this technology. Our finished parts were sturdy, functional, and modifiable with common hand tools. The 3D printer was a valuable resource for our team, and it is recommended that future MQP teams also take advantage of this technology.

Experiments

A number of different kinds of tests were conducted with our prototype parachutes. The following sections discuss these tests in more detail.

Drop testing

Experiments were conducted to determine the descent characteristics of our preliminary cross parachute, and to compare its real-world performance to that predicted by theory. It was dropped from a window on the fourth floor of Salisbury Laboratories on the WPI campus, from approximately 42 feet AGL. The cross parachute had an area of 482 in^2 (0.311 m^2), which would give a predicted descent velocity, with a payload of 1.3 lb (5.8 N) and drag coefficient as determined in the wind tunnel (see following section), of

$$V=\sqrt{\frac{2\cdot D}{\rho\cdot C_D\cdot S_o}}=\sqrt{\frac{2\cdot 5.8}{1.25\,{}^{kg}/_{m^3}\cdot 0.557\cdot 0.311 m^2}}=7.3\ m/s=23.9\ ft/s \qquad \text{Eq. 13}$$

This calculated value reasonably corresponds to the measured descent velocities of approximately 22 to 25 ft/s with this payload weight. The measured velocity was determined as follows:

1. Ten-megapixel digital photographs of the descending parachute were taken in high-speed continuous burst mode on a Nikon D200 digital camera. A tape measure with one-foot increments marked on it was positioned behind the descending parachute.

2. The digital camera has an advertised rapid-fire rate of 5 frames per second (fps). This number was verified as 0.199 sec/frame (or 5.025 fps) with an audio recording and the audio editing software Adobe Audition as shown in Fig. 29.

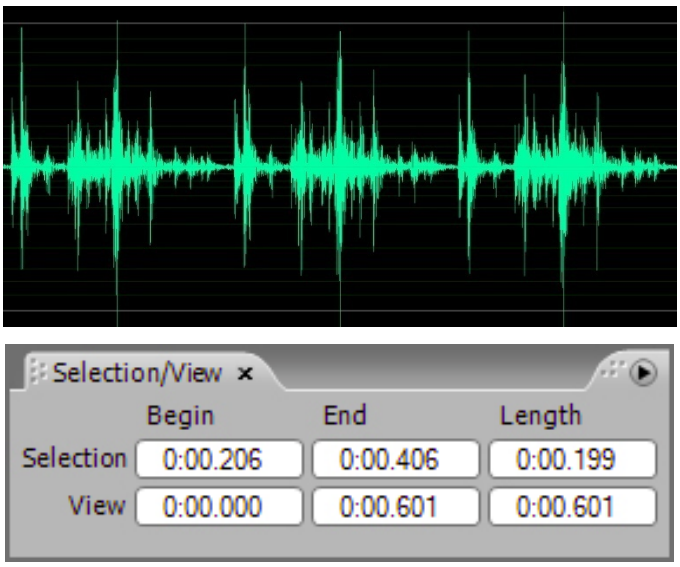

Figure 29: Screen captures from Adobe Audition showing the audio waveform for three consecutive frames in high speed burst mode (top) and the reported time between frames (bottom)

3. Successive frames from the end of each drop test, when the parachute was at or near terminal velocity, were examined in Adobe Photoshop, and the distance the parachute fell between frames was approximated. In this particular drop, the parachute falls approximately 4.25 feet between two (digitally overlapped and enhanced) frames. The yellow lines were drawn in Photoshop at the level of each white mark on the tape measure, to assist with distance estimation.

Figure 30: Drop test distance estimation, with frame overlap and enhancement done using Adobe Photoshop

4. The velocity of the parachute, therefore, is the distance divided by the time between frames. For example, 4.25 feet / 0.199 seconds = 21 ft/s.

While this method lacked precision, it was sufficient for the purposes of determining the parachute's descent velocity to within one or two feet per second. Figure 31 depicts the cross parachute's descent as a series of images, each 0.199 seconds apart.

Figure 31: Cross parachute descent sequence; canopy circled in each frame

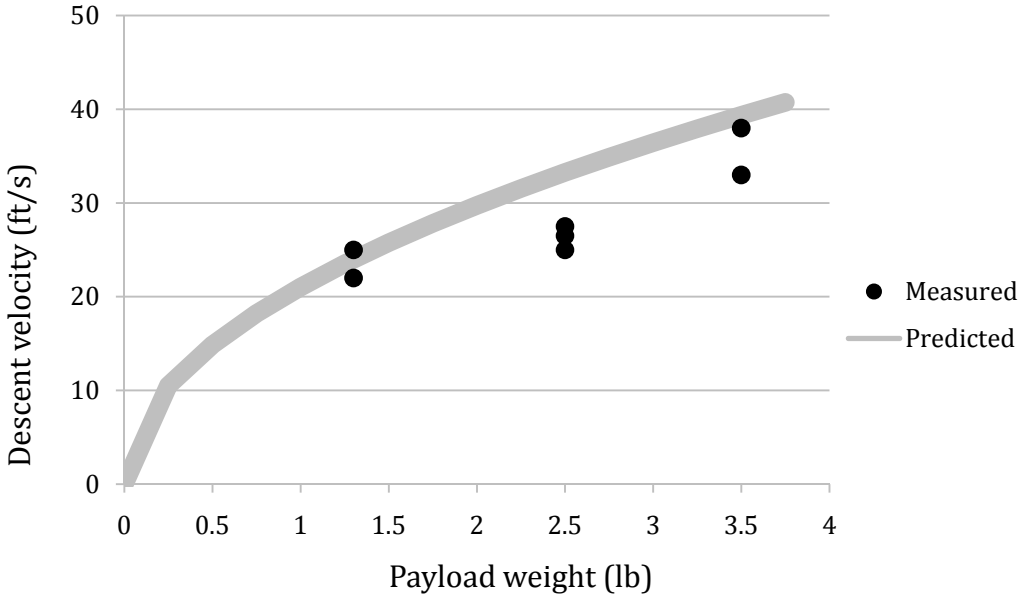

Figure 32: Actual recorded descent velocities compared to predicted values

Drop testing led us to discover an error in our preliminary design sizing calculations, likely resulting from the use of a non-metric unit system; we had aimed for a descent velocity of 8 ft/s, but were recording values in the range of 20 to 30 ft/s. No harm was done at this early stage, however, and we learned to be more careful with units and conversions in future design calculations.

Cross parachute drop tests were conducted over two days. The results are summarized in the plot in Fig. 32 and in Table V.

Table V: Summary of cross parachute drop test results

Date and time	Conditions	Test #	Payload weight	Descent velocity
November 12, 2008, 2pm	Air temperature: 42°F Pressure: 1027.7mb	1	1.3 lb	25 ft/s
		2	1.3 lb	22 ft/s
		3	3.5 lb	33 ft/s
		4	3.5 lb	38 ft/s
November 13, 2008, 1pm	Air temperature: 42°F Pressure: 1024.2mb	5	2.5 lb	25 ft/s
		6	2.5 lb	27 ft/s
		7	2.5 lb	26 ft/s

Figure 33: Dropping the cross parachute from the fourth floor of Salisbury Laboratories at WPI

In addition to drop tests of the prototype cross parachute, drop tests were also conducted with the final prototype sailwing and parafoil canopies. No useful data were obtained from these tests, there not being enough time for either canopy to inflate from such a low drop altitude. Drop tests for the parafoil and sailwing are shown in Fig. 34.

Figure 34: Drop testing the parafoil (left) and the sailwing (right) from Salisbury Labs

Wind tunnel testing

To ensure that the C_D for our cross parachute was accurate, we tested the canopy in WPI's closed circuit wind tunnel. The wind tunnel has a 2 ft x 2 ft x 10 ft test section, a contraction ration of 6:1, and a maximum speed of 55 m/s. The force balance system that we used was an Aerolab Sting Balance, which had a maximum axial force load rating of 10 lbf, and a measurement resolution of 0.01 pounds. The force balance was set up facing the oncoming wind with the parachute trailing behind (illustrated in Fig. 35). This was done in order to obtain positive drag force readings. The opened parachute had a cross sectional area of 0.84 ft^2, which gave our experiment a blockage of 21%. The suggested value for blockage is less than ten percent, but in practice, values often range above this number, as did ours.

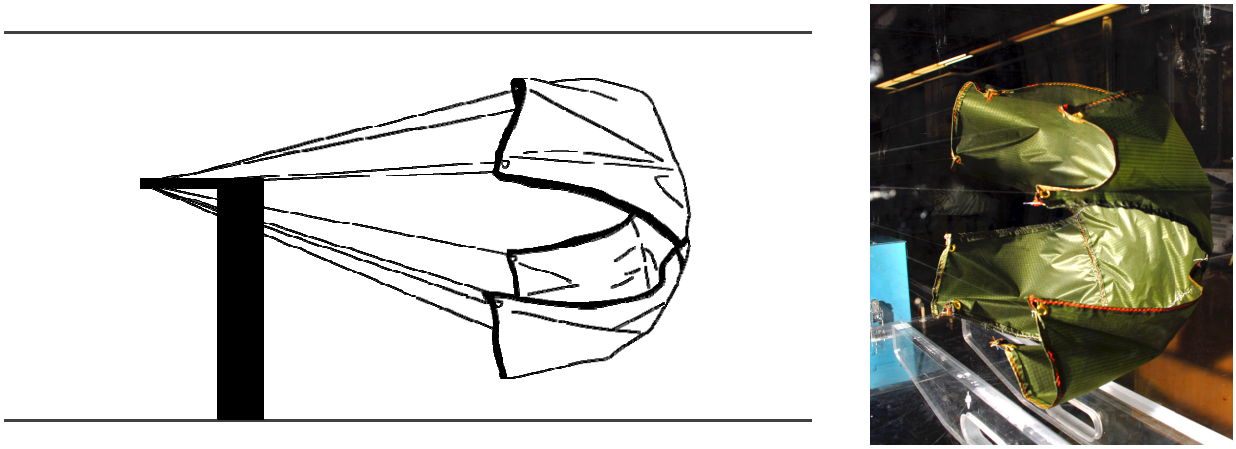

Figure 35: Cross parachute on force balance, illustration and photograph

For the test, we started the tunnel at a medium velocity (around 4 m/s) in order to ensure that the parachute was inflated, and then decreased the speed to a lower velocity (2 m/s). Once the velocity was decreased to this level, the parachute slightly deflated, and rested on the bottom of the wind tunnel test section, producing a drag force of zero pounds. Because of this failure to stay inflated, the velocity was increased to 3 m/s, and subsequently to 3.5 m/s to ensure that readings accurately represented the forces produced by the parachute. After 3.5 m/s, we increased the wind tunnel velocity in increments of 0.1 m/s, which was the smallest increment that the wind tunnel allowed.

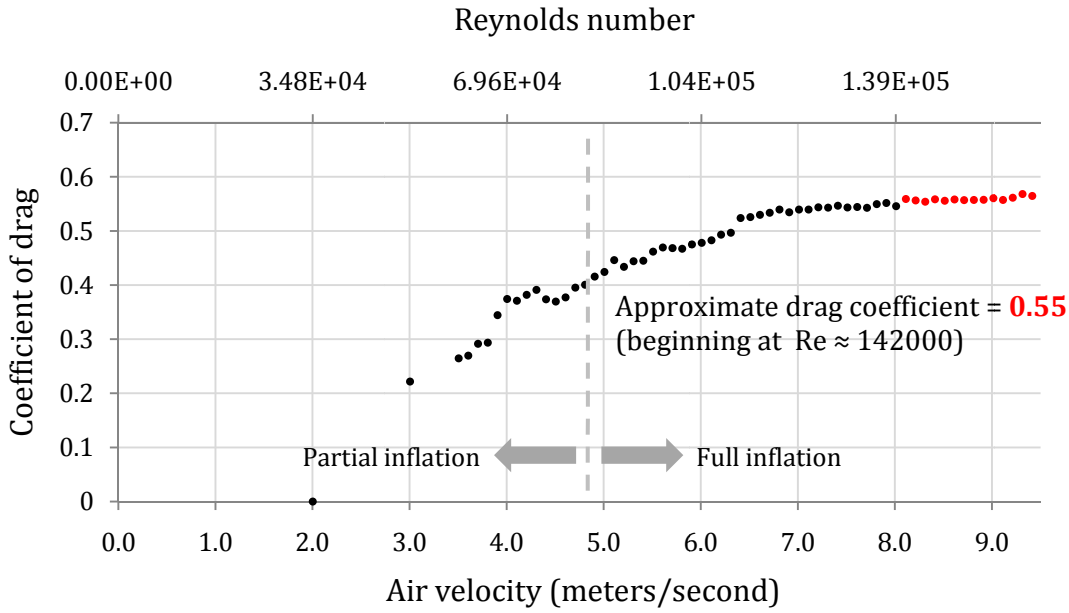

Figure 36: Graph of C_D vs. air velocity and Reynolds number

Our cross parachute's C_D varied with increasing wind speed, as shown in Fig. 36, but several variables must be considered to account for this. First, the cross parachute was not fully inflated until the air velocity was 4.9 m/s, which is roughly where the C_D values become less variable. The parachute exhibited some tendencies to "bounce" off of the bottom of the wind tunnel test section after fully inflating, and continued until an air velocity of 6.2 m/s, possibly causing more variability. At 7.0 m/s wind velocity, the parachute showed some tendency to oscillate vertically about its center point, but stopped when the velocity reached 7.3 m/s, where, once the Reynolds number for the parachute reached 1.12×10^5, the C_D values started to plateau, and finally ceased to change around Re = 1.42×10^5. Taking the average of the values on the plateau, we calculated a C_D of 0.557, which is slightly lower than the lowest value of 0.6 (as determined by Knacke).

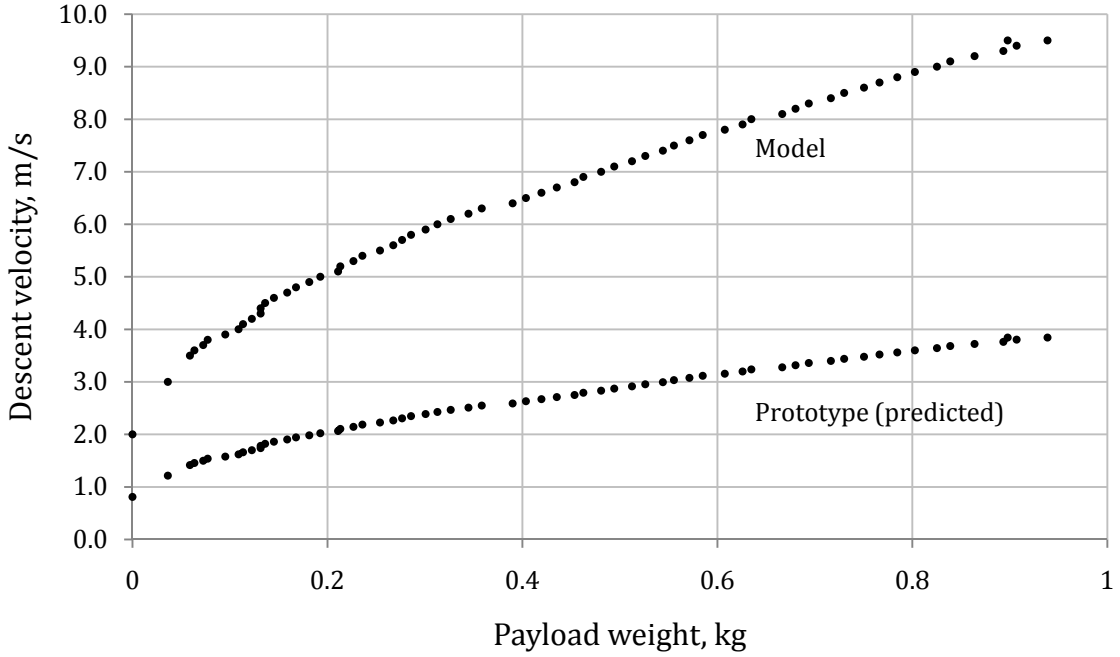

Figure 37: Graph of descent velocity as a function of payload weight

The model parachute that we tested in the wind tunnel had a total surface area of 0.311 m^2 and an inflated diameter of 0.277 m. The convention introduced by Knacke for parachute testing is to use the total surface area of the parachute in calculating the coefficient of drag. For parachutes at terminal velocity, the decent velocity is governed by the equation

$$W_P = D = \frac{1}{2}\rho V^2 S_0 C_D \quad \text{Eq. 14}$$

where W_P,the weight of the payload, is equal to D, the drag produced by the parachute. Using this equation in culmination with Reynolds number similarity, we were able to plot W_P vs. the drop velocity of the model parachute and predict the drop velocities of the prototype, as shown in Fig. 37. Reynolds number is defined as

$$Re = \frac{\rho VD}{\mu} \quad \text{Eq. 15}$$

where μ is the kinematic viscosity of air. For parachutes, it is acceptable to equate the Reynolds numbers of models and prototypes ($Re_{model} = Re_{prototype}$) in order to predict the behavior of the full-sized parachute. For our prototype cross parachute, the inflated diameter was 0.686 m.

Fan testing

Because of our wind tunnel's size limitations, and the inadequate drop times provided by building drop tests, we also used an industrial fan to test our parachutes in a somewhat controlled air flow. The fan, manufactured by Utilitech, was 36 inches in diameter. The speed control on the fan was labeled “high” and “low,” and we were not able to quantify any reliable wind speeds associated with these settings. In an effort to channel the flow and make it more concentrated and laminar near the fan, we added an 18-inch cardboard extension protruding from around the circumference of the fan.

Despite our efforts, we found the fan flow to still be turbulent, so it was not practical to take record any quantitative data from these tests. We instead used the fan to test for canopy instabilities, to set line lengths, and to correct inflation problems. The fan was primarily used on its side with the airstream almost parallel to the ground, and also while lying flat over two chairs, to provide a vertical air flow. Having access to these two types of flow allowed for different testing applications, including both modes of both canopies. The majority of our tests were done with the flow perpendicular to the ground, but we also

used the sideways flow to set the parafoil's line lengths (see Fig. 38). This was done by placing the parafoil upside down in front of the fan, and then adjusting the lengths of the lines until the greatest lift was achieved. The line lengths for the sailwing were set by holding it over the vertical fan flow and changing the relative lengths of its rigging lines to maximize its inflation (Fig. 38). This method was also used to set the line lengths for the cross and round parachutes (Fig. 38).

In addition to testing with a fan, some other qualitative tests were done outside in a walkway between two buildings that frequently channel the wind at high speeds, an area of the WPI campus colloquially known as the "Wind Tunnel." These tests mostly involved checking for inflation problems in the parachutes, as shown in Fig. 39.

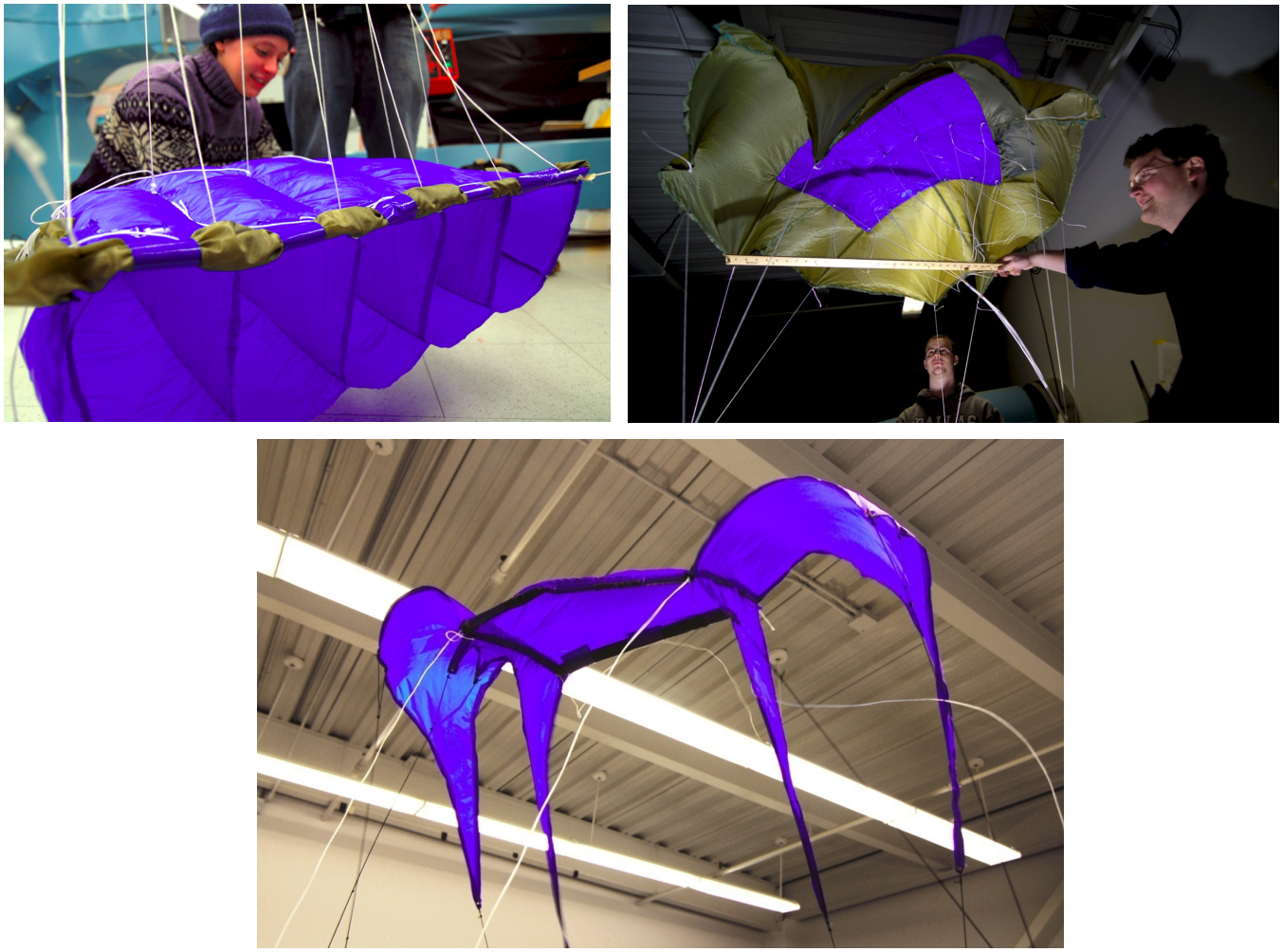

Figure 38: Setting line length for the parafoil (top left), round parachute (top right), and sailwing (bottom).

Figure 39: Sailwing/cross parachute testing in an outdoor, semi-channeled flow

Helicopter drop test

Several months into the construction and testing phase of our project, after both canopy prototypes had been fully constructed, our sponsor extended the offer of a true drop test from an altitude unachievable in any campus building.

Background

It was suggested that we make some alterations to our canopies such that they would be able to be thrown from a UH-60 Black Hawk helicopter at the U.S. Army's Flintstone Drop Zone in West Warwick, Rhode Island (lat./long.: 41° 38' 38" N, 71° 34' 42" W). We readily accepted and set a date for the drop, April 16, 2009. Before the test, however, our sponsor required us to make several modifications to the canopies, most pertaining to safety issues associated with the use of a helicopter as the drop vehicle.

While the plan all along was to use a helicopter for the test, it would have theoretically been possible to have used an actual military cargo aircraft instead. Because of uncertainties about quality of craftsmanship in our canopies, however, and the high deployment speeds (around 110 knots) involved with a fixed-wing drop, a drop from a stationary helicopter was preferred by all parties.

Figure 40: The payload package on the parafoil (identical to the sailwing's). Sandbag is olive green, receiver is red, battery is bright green, and servo-mechanism is black and white.

While both our canopies were designed for a payload in the range of 1 to 2 lbs, our sponsor required the systems to have more mass. Unofficial Army experiments had been conducted with helicopters and lightweight payloads before, and objects weighing less than 1 lb were frequently caught in the suction of the tail rotor and destroyed. As such, we were required to add mass to our payload, in the form of plastic sandbags. Two bags, each weighing 2.5 lbs, were constructed by our sponsor and secured to our payload base. The entire payload package used for each canopy during the drop is shown in Fig. 40.

The addition of extra payload weight would mean our canopies would operate with a much steeper glide slope than originally intended. While this would be undesirable in real-world applications, it was actually a preferred behavior for the drop test, because it would mean the canopies would not travel as far, horizontally, from the point of deployment, making recovery after the test easier.

We were also warned of the violent nature of parachute deployment during initial inflation. In an effort to overcome inflation turbulence that we feared could cause a premature transformation, we strengthened the forces of the magnets securing the post-transformation fabric in place.

A final revelation was that parachutes are not simply "thrown out of" aircraft. Rather, they are packed into a "deployment bag," which is anchored to the helicopter by a static line about 15 feet long. As the parachute is dropped, it remains packed in the bag until the static line is fully extended, at which point the canopy is pulled out by the inertia of the payload, and subsequently inflates. To allow proper deployment from the bag, we packed our parachutes in such a way as to prevent interference between different sets of transformation magnets. The deployment bags used for our canopies were approximately 8 inches long and were standard Army bags used for small drogue parachutes. The parafoil can be seen packed into its deployment bag prior to the drop in Fig. 41.

Figure 41: The parafoil packed into its deployment bag (left) and the sailwing immediately after deployment from its bag at the end of the static line (right)

A virtual non-issue was the possibility of interference between our systems' radio-control servo-mechanisms and the helicopter's avionics. After a quick check with our sponsor, no problems were predicted, nor were any encountered during the test.

Prior to the actual test, we made a trip to visit our sponsor and have the canopies inspected and packed. Our preparatory work on the canopies was deemed satisfactory, and

an in-person discussion of the test helped prepare all parties involved for the unique logistics involved in the deployment of our parachutes.

Test conditions

Figure 42: The Black Hawk arrives in weather conditions ideally suited to the test

The test took place on Thursday, April 16 at around 10am. The weather at the drop zone was sunny and 46°F, with winds from the north at around 16 mph. The helicopter, piloted by Colonel Christopher Callahan and Chief Warrant Officer Mark Iannuccilli and with Natick engineer Jim Sadeck aboard to act as loadmaster, landed to arrange radio communication with the ground, as well as to pick up our canopies. Moments before lift-off, a radio control issue had been discovered that was preventing communication with one of the servo-mechanisms. However, we were able to resolve the issue in time, and both canopies, the parafoil now fully functional, were loaded onto the helicopter.

Sailwing helicopter test

The first canopy to be deployed was the sailwing, from an altitude of around 300 feet above ground level. Video captures show a total time in the air for the sailwing of 10.2 seconds, at a roughly constant velocity. This indicates an average descent velocity of 29.4 ft/s, which compares to an ODE-predicted terminal velocity of 25.2 ft/s with a total system mass of 3.3 lbs (1.50 kg). Unfortunately, immediately after deployment, the sailwing appeared to have transformed prematurely. We suspect this was because of inadequate magnet strength, despite our efforts to increase the force in the preceding days. As predicted by our sponsor, the shock of the deployment was enough to cause the transformation to take place without being properly triggered. Images of the sailwing's descent entirely in post-transformation mode can be seen in Fig. 43.

Figure 43: A series of images showing the sailwing as it descends in post-transformation mode

While the transformation took place immediately and without our having triggered it, we note here that the sailwing was properly packed into its deployment bag in pre-transformation mode by a professional parachute rigger, and that therefore the transformation occurred correctly and without any complications, but simply at the wrong time.

Regardless of the disappointment of a premature transformation, the sailwing functioned perfectly in its post-transformation mode, as a cross parachute. Possible problems with the cross parachute design (e.g., oscillation, rotation) did not manifest themselves, and the payload was delivered to the ground undamaged and in perfect condition to be reused, should it have been necessary.

Parafoil helicopter test

Following the sailwing drop, a wiring problem was identified on the parafoil by the helicopter crew, leading to a brief landing to have the team rectify it. The helicopter then took off and returned to an altitude of around 300 feet, after which the parafoil was deployed from its deployment bag. Videos showed a total time in the air of 10.2 seconds. This translates to an average descent velocity of 29.4 ft/s, which compares to a predicted value of 22.0 ft/s with the systems' total mass of 3.6 lbs (1.65 kg).

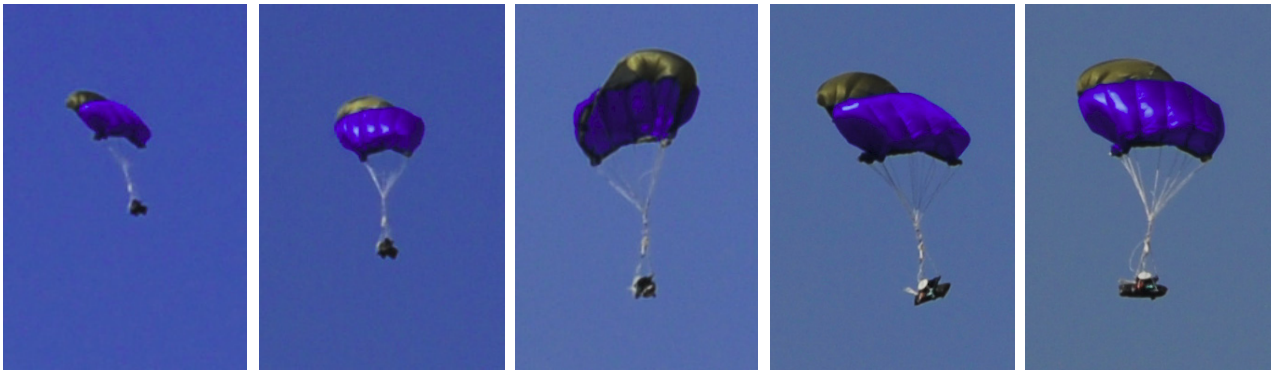

Figure 44: A series of images showing the parafoil as it descends in pre-transformation mode with a portion of post-transformation fabric partially deployed

Like the sailwing, the parafoil also encountered a technical problem that prevented a controlled transformation. Video and photographic replays show the canopy rotating as it leaves the helicopter, a behavior likely caused by some combination of wind, rotor wash, and the variable and unpredictable nature of the jerk freeing the canopy from its deployment bag. In any event, the rotation appeared to lead to twisting of the pre- and post-transformation lines around each other, resulting in friction that, we speculated, prevented the payload from dropping properly at the moment of transformation.

After recovery, inspection of the parafoil indicated that this conclusion was correct; the sets of lines were twisted around one another, and despite the servo having correctly rotated to trigger the transformation, all but two magnets along the trailing edge remained attached, and the round parachute never unrolled as intended. A series of images illustrating the parafoil's descent can be seen in Fig. 44.

Figure 45: From left, the team consisting of Kyle Miller, Jeffrey Moffett, Casey Rogan and Amanda Pollack, with the sailwing (left) and the parafoil (right) in good condition after the helicopter drop test.

IV. CONCLUSIONS

This project was a challenging, multifaceted undertaking that served as the culmination of four years of undergraduate aerospace education. It included aspects in design, fluids, mechanical processes, materials, fabrication and prototyping, lab testing, and field testing. Despite challenges in many areas, the team was able to complete its main objective by designing and constructing two working parachute canopies that, under ideal conditions, can both transform from a high- L/D gliding canopy to a low-L/D canopy.

While neither canopy transformed as desired during the helicopter drop test, we remain pleased with the results. For one, this final test nevertheless consisted of, in many respects, a number of "firsts" for our canopies: first drop from any appreciable altitude, first attempt at transformation in a free stream, first deployment from a bag, first time either canopy reached terminal velocity, and so on. Given the parachute engineer's reliance on Murphy's Law ("anything that can go wrong during a parachute drop, will"), we didn't realistically expect perfection in either of the single drops our canopies were given.

Furthermore, both canopies did appear to be on the right track for a successful transformation. The sailwing transformed flawlessly (but at the wrong time), and the parafoil transformed partially and likely would have completed its transformation had the lines not been twisted and the payload able to drop as intended. Both our canopies did, in fact, fly successfully as parachutes. Given that we constructed both canopies entirely on our own, largely without access to plans or instructions, we were gratified to watch both parachutes inflate and descend to the ground at a velocity far slower than free-fall, with both payloads surviving unscathed, as shown in Fig. 45.

Future recommendations

Our work on this project has led us to create a list of recommendations for continued work in the field of transforming parachutes.

Scale up to 5 lbs or greater

Our canopies were limited in size because of limited fabric supplies and other practical testing considerations. Larger canopies and payloads could be of more practical use in both military and commercial sectors; however, a redesign of the transformation mechanism may be necessary prior to large-scale implementation.

Construct canopies professionally

Constructing parachute canopies with little to no sewing experience was a risk that ended surprisingly well. Outsourcing the construction and assembly of the canopies to experienced professionals would greatly reduce the number of variables affecting the flight performance of the canopies, also permitting more careful studies of flight dynamics to be conducted.

Implement GPS control

Our system currently has no means of steering itself or triggering the transformation autonomously. Before our system could replace any current system, these features would need to be developed, or current mechanisms adapted to our new type of canopy.

Prevent tangling

Overall inexperience with parachute rigging may have led us to create canopies more prone to tangling than normal. The necessity of two sets of lines in our implementation adds to the overall rigging complexity of our transforming canopies, but tangling problems could be overcome in the same manner as on current large-scale systems.

Test in large wind tunnels

Limitations in WPI facilities prevented us from testing either final canopy in a closed wind tunnel. While our interim solution consisting of an industrial fan was reasonably successful, much more detailed studies of our canopies' aerodynamic performance could be done in the controlled flow of a large wind tunnel.

Conduct extensive drop tests

The drop test from the helicopter was an excellent final test for our canopies, but it also resulted in many new questions about the canopies' performance and capabilities. Access to a tall structure, preferably one already in use for parachute testing, would permit troubleshooting and a much greater opportunity to apply trial and error in identifying and solving problems.

REFERENCES

1. "Screamer Precision Cargo Delivery System," Strong Enterprises, Florida, 2006. [http://www.strongparachutes.com/pages/mil_screamer_cargo.php. Accessed 10/05/08]

2. Knacke, T.W., *Parachute Recovery Systems Design Manual*, Para Publishing, California, 1992.

3. Lucas, J., *The Big Umbrella*, Drake Publishers Inc., New York, 1975.

4. Berg, A.S., *Lindbergh*, G. Putnam's Sons, 1998.

5. "Qinetiq Subsidiary's Pricision Airdrop System Used by USAF in Afghanistan," SpaceDaily. AFP, Afghanistan, 2006. [http://www.spacedaily.com/reports/Qinetiq_ Subsidiarys_Precision_Airdrop_System_Used_By_USAF_In_Afghanistan_999.html. Accessed 11/21/2008]

6. Walsh, P., "Joint Precision Airdrop Takes Flight," The Warrior Winter 2006, U.S. Army Soldier Systems Center (Natick), 2007. [http://www.natick.army.mil/about/pao/pubs/warrior/07/index.htm#a4. Accessed 11/21/2008]

7. "Two Sherpas Fielded in Iraq," The Warrior September-October 2004, U.S. Army Soldier Systems Cener (Natick), 2004. [http://www.natick.army.mil/about/pao/pubs/warrior/04/septoct/index.htm#a1. Accessed 11/21/2008]

8. Majewski, A.R., and CPT Pack, A.A., "Precision Cargo Air Drop – Coming to Your Servicing Theater," Quartermaster Professional Bulletin, U.S. Army Quartermaster Center and School, 2004. [http://www.quartermaster.army.mil/oqmg/Professional_Bulletin/2004/Winter04/ Precision_Cargo_Air_Drop_Coming_to_Your_Servicing_Theater.htm. Accessed 10/07/08]

9. Kazmierski, M.J., "It Maneuvers A Battalion: Light Mechanized Delta Anti-Tank Company Moves Alpha, Bravo and Charlie Companies Under Armor," Airborne Warfare, 1990. [http://www.combatreform.com/itmaneuversabattalion.htm. Accessed 11/21/2008]

10. Kendrick, R.S., "Joint Logistics for the EUCOM AOR-Part II," Army Logistician, 2006. [http:// www.almc.army.mil/alog/issues/JanFeb06/EUCOM_aor_2.html. Accessed 11/21/2008]

11. "Airdrop Systems," GlobalSecurity.org, John Pike, 2008. [http://www.globalsecurity.org/ military/systems/aircraft/systems/airdrop.htm. Accessed 10/7/08]

12. "The US Army Quartermaster Air Delivery Units and the Defense of Khe Sanh," Vietnam Airdrop History, 2007. [http://www103.pair.com/adsd/riggers/main3.html. Accessed 11/21/2008]

13. Babbar, Y., "Computational Analysis of Ram Air Parachute Canopy Using Panel Methods," Punjab Engineering College, Chandigarh, 2004. [www.casde.iitb.ac.in/Publications/pdfdoc-2004/ictacem-yb-2004.ppt. Accessed 12/07/2008]

14. "Air – Density and Specific Weight," The Engineering Toolbox, 2005. [http://www.engineeringtoolbox.com/air-desity-specific-weight-d_600.html. Accessed 12/07/2008]

15. "Parachute Recovery Systems," The Rocketry EGGsploration Challenge. [http://www.eggsploration.org/downloads/trec_parachuterecoverysystems.pdf. Accessed 12/08/2008]

16. Potvin, Dr. J., "Calculating the Descent Rate of a Round Parachute," Parks College Parachute Research Group. [http://www.pcprg.com/rounddes.htm. Accessed 12/08/2008]

17. Ginzburg, I., "Photography," 2009. [www.murblanc.org. Accessed 12/07/2008]

18. Murillo, X., "David Barish, the forgotten father of paragliding," Cross Country Magazine, 2001. [http://www.flyaboveall.com/articles/davidbarish.htm. Accessed 12/07/2008]

19. "Barish Sailwing," ParachuteHistory.com, 2003. [http://www.parachutehistory.com/other/sailwing.html. Accessed 12/07/2008]

20. Roti, S., "Interview with David Barish," United States Hang Gliding and Paragliding Association, Inc, 2008. [http://www.ushpa.aero/article.asp?id=29. Accessed 12/07/2008]

21. Daoust, J., "Paragliding's Believe it or Not, " 2008. [http://www.expandingknowledge.com/Jerome/PG/History/Strange/Album.htm. Accessed 12/07/2008]

22. "Flight with a Sailwing," Air Adventure, 2008. [http://www.air.aventure.free.fr/infos_barish.htm. Accessed 12/07/2008]

23. Weiberg, J.A., and Mort, K.W., "Wind-tunnel tests of a Series of Parachutes Designed for Controllable Gliding Flight," NASA TN D-3960, May, 1967.

24. Ware, G.M., and Libbey, C.E., "Wind-Tunnel Investigation of the Static Aerodynamic Characteristics of a Multilobe Gliding Parachute," NASA TN D-4672, July, 1968.

25. Eilertson, W.H., "Gliding Parachutes for Land Recovery of Space Vehicles Case 730," NASA-CR-108990, September, 1969.

26. Forostoski, M., Riley, J., Vaillancourt, V., and Wilfong, J., "Investigation of Variable-Glide Parafoils," Worcester Polytechnic Institute Major Qualifying Project, 2006.

27. Meade, D. B., *ODE Models for the Parachute Problem*, SIAM Review, Vol. 40, Issue 2, pp. 327-332, June 1998. [http://www.math.sc.edu/~meade/msw2004/Parachute/sr-parachute.pdf. Accessed 2/12/2009]

28. "Dimension 1200es Series: Product Specification," Dimension, 2009. [http://www.dimensionprinting.com/3d-printers/printing-productspecs1200series.aspx. Accessed 12/10/2008]

29. "3D Printers: Frequently Asked Questions," Dimension, 2009. [http://www.dimensionprinting.com/3d-printers/3d-printing-faq.aspx. Accessed 12/10/2008]

30. "Product Features," Dimension, 2009. [http://www.dimensionprinting.com. Accessed 12/10/2008]

APPENDIX

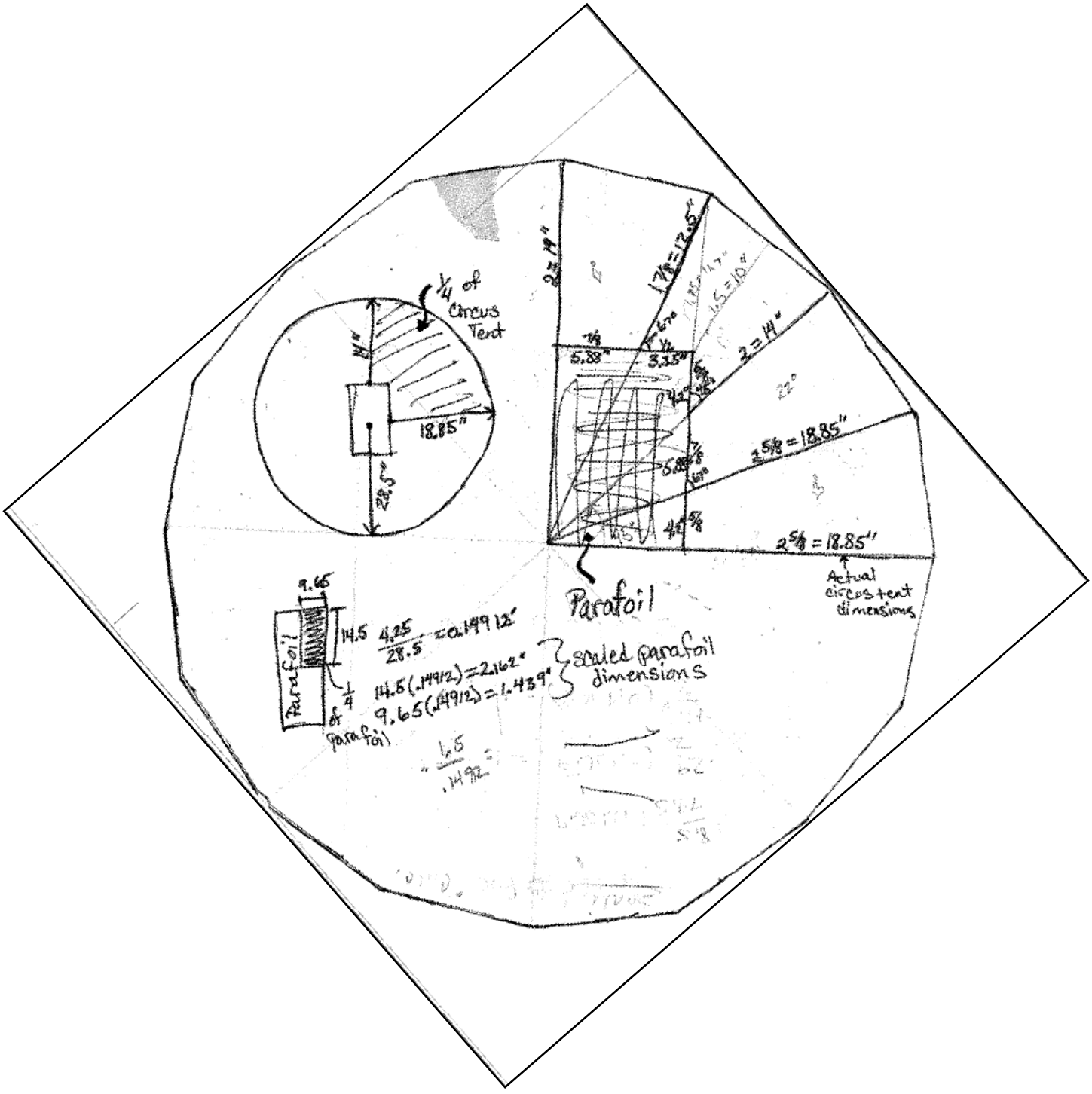

On this page: the post-transformation parafoil pattern before being scaled up to size.